CHALMERS
UNIVERSITY OF TECHNOLOGY

Performance based standards for heavy vehicle combinations with electrified dolly

Master's thesis in Mobility Engineering

Aakash Rishi

DEPARTMENT OF MECHANICS AND MARITIME SCIENCES
CHALMERS UNIVERSITY OF TECHNOLOGY
Gothenburg, Sweden 2023
www.chalmers.se

Master's thesis 2023

Performance based standards for heavy vehicle combinations with electrified dolly

AAKASH RISHI

CHALMERS
UNIVERSITY OF TECHNOLOGY

Department of Mechanics and Maritime Sciences
Division of Vehicle Engineering and Autonomous Systems
Chalmers University of Technology
Gothenburg, Sweden 2023

Performance based standards for heavy vehicle combinations with electrified dolly
AAKASH RISHI

Examiner: Fredrik Bruzelius, Department of Mechanics and Maritime Sciences
Supervisor: Bengt Jacobson, Department of Mechanics and Maritime Sciences

Master's Thesis 2023
Department of Mechanics and Maritime Sciences
Division of Vehicle Engineering and Autonomous Systems
Chalmers University of Technology
SE-412 96 Gothenburg
Telephone +46 31 772 1000

Typeset in LaTeX
Printed by Chalmers Reproservice
Gothenburg, Sweden 2023

A Performance Based Standard for electrified dolly combinations
AAKASH RISHI
Department of Mechanics and Maritime Sciences
Chalmers University of Technology

Abstract

The need to create environmentally friendly transport solutions has guided research in vehicle engineering over the past few decades. As a result, Battery Electric Powertrains are now in operation in small vehicles like cars. However, these solutions often fall short in terms of providing long mission ranges and high payload capacity. Consequently, implementing them independently in Long Combination Vehicles (LCVs) presents a challenge. This situation creates an opportunity to explore longer and heavier High Capacity Transport (HCT) vehicles, which could reduce the number of trips required. These HCTs could potentially feature hybridized powertrains with multiple propelling units, at least for the time being.

However, the use of multiple propelling units is likely to have an impact on vehicle dynamics, particularly in the areas of braking stability and traction capability. This effect could potentially lead to instability issues, such as jack-knifing. Therefore, to ensure their compliance with street regulations, it is imperative to analyze their performance based on the tests outlined in the Performance Based Standards (PBS) framework.

The HELPED project has been exploring the integration of electrified dollies in A-double HCT combinations. This thesis work falls within the scope of this project and seeks to address several questions: How does the performance of an electrified A-double differ from that of a conventional one in terms of vehicle stability and traction when subjected to specific PBS tests? Is the existing PBS framework sufficient to ensure the safe operation of an electrified dolly? If necessary, what additional tests might be required to assess and establish legislation for electrified dolly combinations?

To address these questions, this thesis work involves modeling an A-double HCT vehicle combination. The investigation includes modeling specific test cases to study the traction capability and stability of the combination with and without an electrified dolly. The simulations encompass maneuvers such as Startability, Gradability, Single Lane Change, and Deceleration in a curve. The results indicate that in terms of traction, the electrified A-double performs significantly better than a conventional one. However, the results from the stability simulations show that in certain conditions, such as when carrying a lighter payload on low-friction surfaces, it performs worse when subjected to aggressive maneuvers. Hence, the implementation of an A-double may require striking a balance between environmental efficiency and safety considerations.

Keywords: Battery Electric Powertrian, Performance Based Standards, Long Combination Vehicle, High Capacity Transport, HELPED, Single Lane Change

Acknowledgements

I would like to thank my Examiner, Fredrik Bruzelius, for providing me the opportunity to work on this project and guiding me throughout the process. I would not have been able to work on this thesis if not for his vision.

I would like to extend my gratitude to Bengt JH Jacboson for helping me with daily problems, and having knowledgeable discussions with me. My knowledge about the core subject matter greatly improved during this work. Special thanks to our contact at Volvo Group Trucks Technology, Dr. Toheed Ghandriz for giving valuable ideas to try and explore with during the work, and helping me validate my work from time to time.

Thanks to all my friends and PhD scholars, at the Division of Vehicle Engineering and Autonomous systems for clearing my doubts and guiding me through some general queries through the process and allowing me to be a part of a healthy workplace. Thanks to Sonja Laakso Gustafsson for helping me with the document formalities and other official work during my thesis. Thanks to Simone Sebben for allowing me to be a part of the division.

Lastly I want to thank my parents for their support to keep me enthusiastic for this work. The work would have been extremely challenging if not for their care and wishes.

Aakash Rishi Gothenburg, August, 2023

List of Acronyms

Below is the list of acronyms that have been used throughout this thesis listed in alphabetical order:

DAE	Differential Algebraic Equations
DIC	Deceleration in a curve
HCT	High Capacity Transport
IC	Internal Combustion
LCV	Long Combination Vehicle
RA	Rearward Amplification
SLC	Single Lane Change

Nomenclature

Below is the nomenclature of indices, sets, parameters, and variables that have been used throughout this thesis.

Parameters

a_i	[m]	Height of the ith coupling point from the ground
C_x	[N/-]	Longitudinal stiffness of the tire
C_y	[N/-]	Cornering stiffness of the tire
CC_x	[-]	Longitudinal slip stiffness coefficient
CC_y	[-]	Lateral slip stiffness coefficient
F_{air}	[N]	Aerodynamic drag force
F_z	[N]	Tire vertical force
F_{zij}	[N]	Axle vertical force at the jth axle of the ith vehicle unit
F_x	[N]	Longitudinal force
F_y	[N]	Lateral force
f_{max}	[-]	Maximum friction usage
g	[m/s^2]	Acceleration due to gravity
G	[N/m^2]	Shear Modulus of rubber
h_i	[m]	Height of the cog of ith vehicle unit from the ground
H	[m]	Tire tread depth
I_i	[Kgm^2]	Yaw moment of inertia
J_w	[Kgm^2]	Wheel rotational inertia
L	[m]	Tire contact patch length
m_i	[Kg]	Mass of the ith vehicle unit
P_{xij}	[N]	Longitudinal hinge force at ith coupling point and on jth unit with respect to the coupling point
P_{yij}	[N]	Lateral hinge force at ith coupling point

		and on jth unit with respect to the coupling point
R	[m]	Wheel Radius
s	[-]	Combined slip
s_x	[-]	Longitudinal slip
s_y	[-]	Lateral slip
T	[Nm]	Wheel Torque
T_{ij}	[Nm]	Axle Torque at the jth axle of the ith vehicle unit
v_{xi}	[m/s]	Longitudinal speed of the ith vehicle unit
v_{yi}	[m/s]	Lateral speed of the ith vehicle unit
W	[m]	Tire contact patch width
ξ_c	[m]	co-ordinate of the break away point
μ_{slip}	[-]	coefficient of slip friction
μ_{stic}	[-]	coefficient of slip friction
α	[rad]	Road grade angle
δ	[rad]	Steering angle at the steered axle
rrc	[-]	Rolling resistance coefficient
ω_{ij}	[rad/s]	Wheel rotational speed of the ith vehicle unit's jth axle
w_{zi}	[rad/s]	Yaw velocity of ith vehicle unit
θ_i	[rad]	Articulation angle at the ith coupling point

Contents

1
Introduction

The world is moving towards sustainable transport solutions. It is clear that the category of small vehicles, such as cars, has seen significant advancements, with Battery Electric Powertrain (BEP) being used in nearly all of its sub-categories. However, for heavy vehicles like buses and trucks, there are certain applications where one can witness BEP in use. For example, buses used for urban transport. However, in the case of trucks, the utilization of BEPs is somewhat restricted due to considerations of both range and payload capacity. For instance, according to Volvo (2023), their FH electric truck has a maximum range of up to 300 kilometers and a Gross Combination Weight (GCW) limit of 44 tonnes [1]. For missions that involve longer distances and heavier payloads, we are still dependent on conventional drivetrains. This segment of vehicles mainly consists of Long Combination Vehicles (LCV), with one or multiple freight-carrying units like trailers, semi-trailers, dollies, etc., coupled to a tractor/truck to form a vehicle train, in which the tractor/truck (propelling unit) acts as the first unit. The current maximum load allowed by the government of Sweden is 74 tonnes and the maximum length is 25.25 meters [3].

Since currently, BEPs cannot be used independently for LCVs, as an initiative to cut down emissions, one can minimize the number of trips by using longer and heavier LCVs to carry more payload per trip. A vehicle combination that is longer and/or heavier than the allowed limit, as mentioned above, is known as High Capacity Transport (HCT) [3]. An HCT could potentially need more powerful drivetrains. Hence, the challenge to cut down on emissions has a potential opportunity to use hybrid powertrain solutions, which could consist of multiple propelling units in a single HCT vehicle combination. However, using this technique is likely to affect the dynamic behavior of the vehicle combination in both positive and negative ways. This motivates a discussion on the legislation to be implemented for such hybrid HCT vehicle combinations.

Over the years, the legislations are set in terms of, what is known as prescriptive manner, in which the dimensions and weights are explicitly controlled. However, over the recent years, another method has come into existence, that addresses the performance of the HCTs. It is called Performance Based Standards (PBS). It is a framework of certain tests for analyzing the performance of the the HCT vehicle in terms of Traction, Stability (Low and High speed), Tracking capability (Low and High speed), and Braking. The performance is measured in terms of certain performance parameters that are specified for each of these categories. For example, Rearward Amplification, Yaw Damping apply for High speed stability whereas, Road inclination is associated with Traction. These parameters are explained later in the

next chapter.

To make a rough comparison between the PBS framework and the prescriptive manner, one could say that in the latter, one prescribes either the weight or the dimensions to the vehicle, knowing one of them already. It is usually based on past experience with vehicles of similar dimensions and mass. But in the PBS, one prescribes the performance requirements that the vehicle should fulfill to be street legal. However, it is not uncommon that certain dimensions are modified for a specialized HCT application. In such cases, predicting vehicle performance using a prescriptive approach becomes difficult. Nevertheless, the PBS approach remains capable of assessing performance even in such scenarios. Thus, the PBS framework is likely to handle the different variants better than the prescriptive manner [4]. The reason for that is slight changes in performance can be noticed with the help of PBS, which is difficult to figure out with the prescriptive manner. So, we have some research questions that guide us to the aim of the thesis.

1.1 Research questions

- In what ways does a hybrid HCT vehicle combination performs better and worse than a conventional HCT vehicle combination?
- Is the current PBS framework enough to analyze the performance of the hybrid HCT vehicle combinations?
- Which additional test maneuvers with measures are proposed for the PBS framework?

1.2 Aim

The aim of the thesis is :-

- To perform tests of PBS framework on an A-double HCT vehicle combination, that contains a dolly converter unit with an electrically propelled axle. This thesis work comes under the HELPED project which proposes the usage of electrified dollies, therefore, in this thesis project, the idea of having multiple propelling units has been kept limited to e-dolly.
- To investigate the need for adding to the existing set of standards in the existing framework.

1.3 Limitations

The limitations of the thesis is :-

- This work is a simulation study. The performance of the vehicle is not studied from the perspective of energy consumption.
- Only an HCT A-double with hybridization through electrification on the 2nd of the 2 axles of the e-dolly, is studied.
- To narrow down the scope of the thesis, not all of the tests maneuvers mentioned in the PBS framework are performed.

1.4 Methodology

- An A-double HCT vehicle combination that contains an electric powered converter dolly unit has been modeled.
- The maneuvers from PBS framework and one other additional maneuver, that are studied, have been modeled as test cases.
- The results are analyzed to understand the vehicle dynamics, and answer the research questions mentioned above.

2
Modeling

In addition to the study of the existing PBS framework and the selection of specific maneuvers for analysis, an essential step in this work is system modeling. The latest version of the open PBS assessment tool [7], known as the OpenPBS package, could not be employed because it was not designed to handle multiple power units within a vehicle combination. Furthermore, the use of IPG Truckmaker was ruled out due to the complexity of our multi-trailer model, which is not readily compatible with combinations comprising more than three units.

An added advantage of building the model from scratch is that it offers better clarity regarding the system's behavior, making it easier to debug and investigate the results. In contrast, utilizing a pre-existing library or package from IPG TruckMaker may not provide this level of insight. Therefore, a new model has been developed from the ground up.

The presence of multiple coupling points in the vehicle combination presents us with a Differential Algebraic Equation (DAE) system. This necessity prompted the use of Dymola software, which incorporates an built-in DAE solver, allowing for the effective handling of DAE systems.

The overall vehicle model comprises subsystems that interact with each other, including the vehicle powertrain (electric motor of the e-dolly), a single-track model for the vehicle units coupled together, and the tire models. In total, there are four vehicle units: the tractor, the first semitrailer, the e-dolly, and the second semitrailer.

The system's properties are defined by parameters such as the coefficients of slip and stick friction, dimensions of the vehicle units like wheelbase, initial speed, mass, power rating of the electric motor, aerodynamic drag coefficient, frontal area (of the tractor), air density, and more. These parameters are used to perform calculations such as determining axle loads and aerodynamic drag forces. For the tires, critical parameters include longitudinal and lateral slip stiffness coefficients (denoted as C_x and C_y), rolling resistance coefficients, and tire radius, among others.

2.1 Tire model

The tire model is used to explain the dependency of the tire forces on the slip, coefficient of friction, and tire parameters like longitudinal and lateral stiffness which are a function of vertical load on the tire as well, etc. For this study, the use of a combined slip brush tire model with a parabolic pressure distribution [8] is

motivated. It can be explained as there are some test maneuvers in which the wheels of the hybrid HCT vehicle combination are subjected to propelling or braking torques while negotiating a turn or changing lanes. This subjects the tires to both longitudinal and lateral slips at the same time and hence leads to forces in both longitudinal and lateral directions. Therefore, it becomes necessary to capture the effects of this combined slip. Secondly, most of the work is carried out for road surface to be dry asphalt. The model with parabolic pressure distribution gives more realistic results for that than the one with uniform pressure distribution.

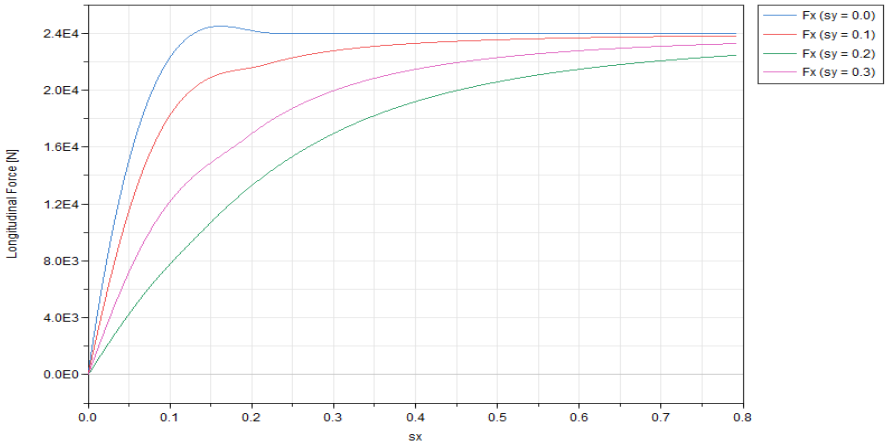

Figure 2.1: Longitudinal force vs longitudinal slip at different lateral slip

But at the same time, there are some simplifications made to the model to make the overall work less complicated.

- The longitudinal and lateral tire stiffness (C_x and C_y) has been assumed to be varying linearly, unlike the real case, where C_y reaches a saturated number if the vertical load > 80 kN.
- The stiction and slip friction coefficients have been assumed to be same in both the lateral and the longitudinal directions.

By taking all the considerations, we can discuss the brush tire model as follows:-
If the combined slip auxiliary parameter s_k happens to be greater than threshold value of $\frac{3 \cdot \mu_{stick} \cdot F_z}{C_y}$, or the $v_x \cdot \omega < 0$, then in that case the entire contact patch slips and we get the respective relations of forces in terms of slip as,

$$\begin{bmatrix} F_x \\ F_y \end{bmatrix} = \frac{\mu_{slip} \cdot F_z}{s} \cdot \begin{bmatrix} s_x \\ s_y \end{bmatrix} \tag{2.1}$$

$$s_k = \sqrt{(k \cdot s_x)^2 + s_y^2} \tag{2.2}$$

But if the s_k value falls within the limits of threshold value, then the expression becomes,

$$\begin{bmatrix} F_x \\ F_y \end{bmatrix} = \begin{bmatrix} C_x \cdot s_x \cdot \left(\frac{\xi_c}{L}\right)^2 + \mu_{slip} \cdot F_z \cdot \left(1 - 3 \cdot \left(\frac{\xi_c}{L}\right)^2 + 2 \cdot \left(\frac{\xi_c}{L}\right)^3\right) \cdot \frac{s_x}{s} \\ -C_y \cdot s_y \cdot \left(\frac{\xi_c}{L}\right)^2 + \mu_{slip} \cdot F_z \cdot \left(1 - 3 \cdot \left(\frac{\xi_c}{L}\right)^2 + 2 \cdot \left(\frac{\xi_c}{L}\right)^3\right) \cdot \frac{s_y}{s} \end{bmatrix} \tag{2.3}$$

Where,

$$s = \sqrt{s_x^2 + s_y^2} \tag{2.4}$$

$$k = \frac{C_x}{C_y} \tag{2.5}$$

$$s_x = \frac{r_w \cdot \omega - v_x}{|r_w \cdot \omega|} \tag{2.6}$$

$$s_y = \frac{-v_y}{|r_w \cdot \omega|} \tag{2.7}$$

$$\frac{\xi_c}{L} = 1 - \frac{C_y \cdot s_k}{\mu_{stic} \cdot 3 \cdot F_z} \tag{2.8}$$

$$C_x = \frac{G \cdot W \cdot L^2}{2 \cdot H} \tag{2.9}$$

In the above set of equations, it is clearly visible that the force generation is a function of the slip and the expression used depends on whether the slip is more than or less than the threshold.
The mathematical representation of the free body diagram of the wheel looks like :-

$$J \cdot (\dot{w_{ij}}) = T_{ij} - F_{xij} \cdot r - F_{zij} \cdot rrc \cdot sign(v_{xi}) \tag{2.10}$$

2.2 Vehicle model

The complete model consists of the model of e-dolly powertrain, one track model of the vehicle units which are coupled together, and tires. In total, there are 4 vehicle units, the tractor, first semitrailer, the dolly, and the second semitrailer.

2.2.1 Tractor

A hybrid powertrain has power distributed over more than one propelled vehicle unit. One is in the tractor, which has an IC Engine and transmission system (gearbox and differential). The other is in the e-dolly which consists of the electric motor and usually only 1 gear ratio as the transmission system between the motor and the driven axle. However, in this investigation, there are some simplifications. Firstly the drivetrain of the tractor is not modeled, and it is assumed that the required power is supplied by the tractor in any case. The reason for doing so is that the aim of the work is to analyze the vehicle dynamics of the combination, which has an e-dolly. The torque supplied by that depends on the vehicle's speed. Hence to capture the effects of e-dolly the electric drivetrain has been modeled.

For the tractor, the dimensions like theoretical wheelbase, and articulation point distance from the front axle, and axle loads are taken from the data-sheet of Volvo FH16 truck [5]. We use these to calculate the location of centre of gravity, and thus compute l_{f1}, l_{r1}, to get the rear axle distances from the front. We use that in the equations of longitudinal and lateral force, and yaw equilibrium of the tractor:

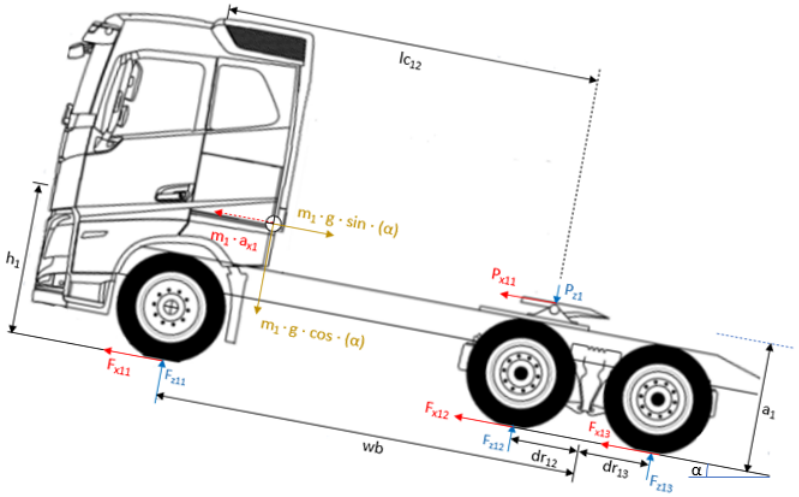

Figure 2.2: Diagram of Tractor

$$m_1 \cdot (\dot{v}_{x1} - w_{z1} \cdot v_{y1}) = F_{x11} \cdot cos(\delta) - F_{y11} \cdot sin(\delta) + F_{x12} + F_{x13} + P_{x11} - m_1 \cdot g \cdot sin(\alpha) - F_{air} \tag{2.11}$$

$$m_1 \cdot (\dot{v}_{y1} + w_{z1} \cdot v_{x1}) = F_{x11} \cdot sin(\delta) + F_{y11} \cdot cos(\delta) + F_{y12} + F_{y13} + P_{y11} \tag{2.12}$$

$$I_{z1} \cdot \dot{w}_{z1} = l_{f1} \cdot (F_{x11} \cdot sin(\delta) + F_{y11} \cdot cos(\delta)) - F_{y12} \cdot (l_{r1} - dr_{12}) - F_{y13} \cdot (l_{r1} + dr_{13}) - P_{y11} \cdot (l_{c12} - l_{f1}) \tag{2.13}$$

Table 2.1: Vehicle parameters of the tractor

Parameter	Description	Length [m]
wb	Theoretical wheelbase	4.085
lc_{12}	Location of the coupling point from the first axle	3.045
a_1	Height of the first coupling point	1.0
h_1	Height of the cog	1.2
dr_{12}	Distance between the 1st rear axle and the center of the rear axle group	0.685
dr_{13}	Distance between the 1st rear axle and the center of the rear axle group	0.685

2.2.2 First Semi-Trailer

The equations of longitudinal and lateral force, and yaw equilibrium semi-trailer 1 are:

$$m_2 \cdot (\dot{v}_{x2} - w_{z2} \cdot v_{y2}) = F_{x21} + F_{x22} + F_{x23} + P_{x21} - m_2 \cdot g \cdot sin(\alpha) + P_{x12} \tag{2.14}$$

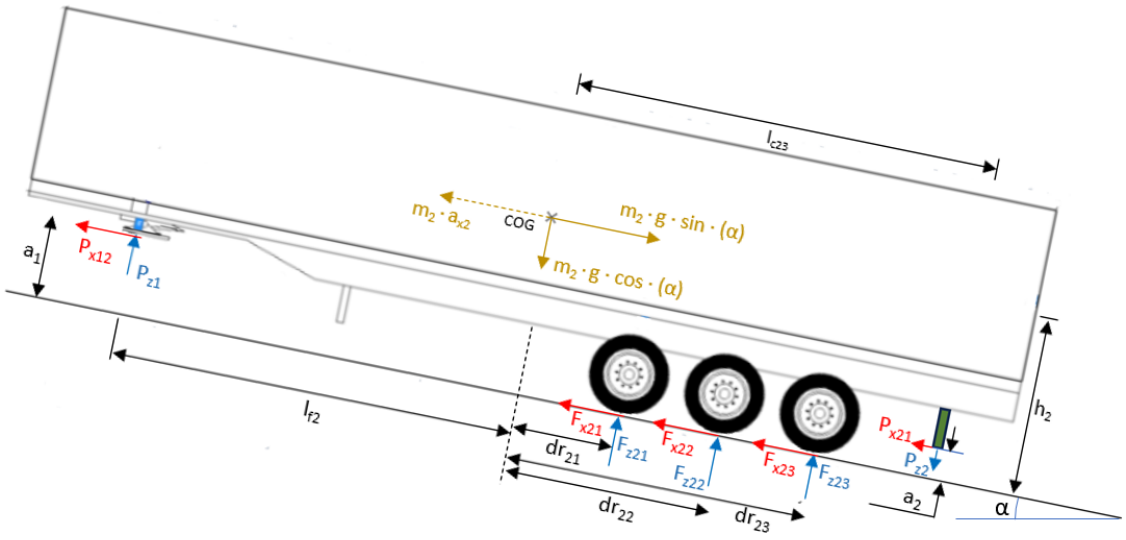

Figure 2.3: Diagram of semi-trailer 1

$$m_2 \cdot (\dot{v}_{y2} + w_{z2} \cdot v_{x2}) = F_{y21} + F_{y22} + F_{y23} + P_{y12} + P_{y21} \tag{2.15}$$

$$I_{z2} \cdot \dot{w}_{z2} = P_{y12} \cdot l_{f2} + P_{y21} \cdot l_{c23} - dr_{21} \cdot F_{y21} - dr_{22} \cdot F_{y22} - dr_{23} \cdot F_{y23} \tag{2.16}$$

Table 2.2: Vehicle parameters for the first Semi-trailer

Parameter	Description	Length [m]
a_2	Height of the second coupling point from the ground surface	1.2
h_2	height of the cog	2.5
lf_2	distance of the cog from the first coupling point	6.32
dr_{21}	distance of the 1st axle from the cog	1.16
dr_{22}	distance of the 2nd axle from the cog	2.47
dr_{23}	distance of the 3rd axle from the cog	3.78
lc_{23}	Distance of the second coupling point from the cog	4.78

2.2.3 Electric Dolly

The model includes an e-dolly that supplies electric power. It can be manually switched on/off. It consists of a DC electric motor which is coupled to the second axle of the dolly via a single gear ratio. For the simulations that have a powered dolly, the switch is turned on. The torque (both propulsive and regenerative) of the motor is a function of motor speed, which can be expressed in 2.4 :-

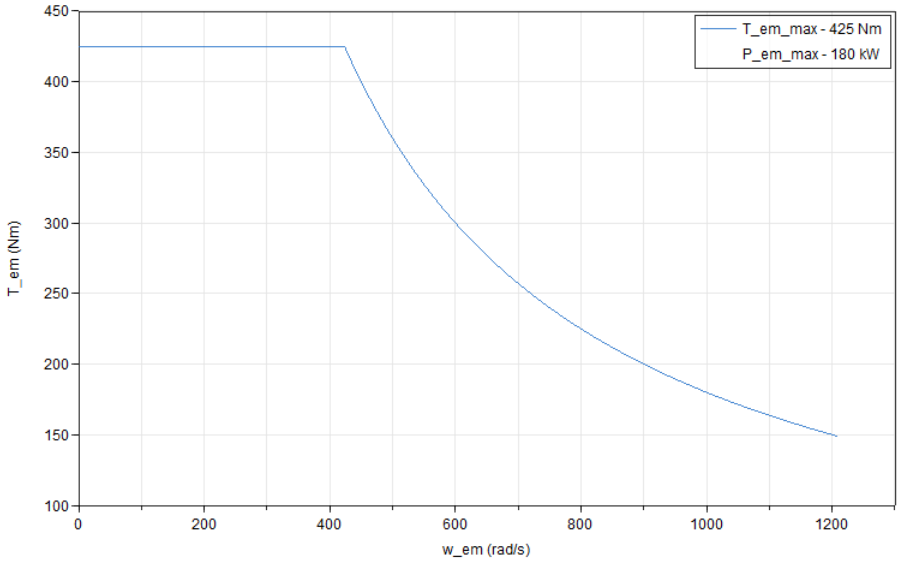

Figure 2.4: Torque-speed curve of 180 kW Electric motor

The data of the electric motor has been taken from [6]. However, to notice the influence of the variation of electric power on the vehicle dynamics, the study has also been conducted with having 2 electric motors housed in the same dolly, to give a total power output of 360 kW.

To limit the complexity of the model of the motor, the rotational inertia has been neglected. Hence the model needs the maximum power, maximum torque of the motor, required vehicle acceleration, and wheel speed of the dolly axle, as input parameters, to determine the torque at the given vehicle speed. Hence the torque allocation to the driven axle of the e-dolly is independent of the torque available at the tractor. The equilibrium equation of the driven axle of the e-dolly becomes:-

$$T_{32} = T_{em} \cdot g_{em} \tag{2.17}$$

$$F_{x32} \cdot r_w = T_{32} - J_w \cdot \dot{\omega}_{32} \tag{2.18}$$

The equations of longitudinal and lateral force, and yaw equilibrium the dolly are:

$$m_3 \cdot (\dot{v}_{x3} - w_{z3} \cdot v_{y3}) = F_{x31} + F_{x32} + P_{x22} + P_{x31} - m_3 \cdot g \cdot sin(\alpha) \tag{2.19}$$

$$m_3 \cdot (\dot{v}_{y3} + w_{z3} \cdot v_{x3}) = F_{y31} + F_{y32} + P_{y22} + P_{y31} \tag{2.20}$$

$$I_{z3} \cdot \dot{w}_{z3} = P_{y22} \cdot l_{c32} + dr_{31} \cdot F_{y31} - dr_{32} \cdot F_{y32} - P_{y31} \cdot l_{c34} \tag{2.21}$$

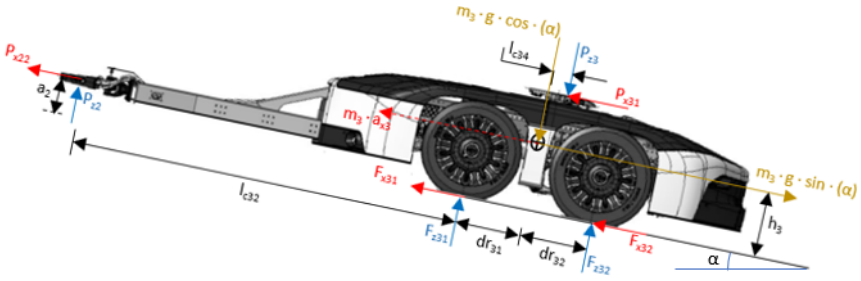

Figure 2.5: Sketch of e-dolly

Table 2.3: Vehicle parameters for the e-dolly

Parameter	Description	Length [m]
lc_{34}	Distance of the third coupling point from the cog	0.6
h_3	height of the cog	0.08
dr_{31}	distance of the 1st axle from the cog	0.66
dr_{32}	distance of the 2nd axle from the cog	0.66
lc_{32}	Distance of the second coupling point from the cog	4.36

Table 2.4

2.2.4 Second Semi-Trailer

The equations of longitudinal and lateral force, and yaw equilibrium of semi-trailer 2 are:

$$m_4 \cdot (\dot{v}_{x4} - w_{z4} \cdot v_{y4}) = F_{x41} + F_{x42} + F_{x43} + P_{x32} - m_4 \cdot g \cdot sin(\alpha) \tag{2.22}$$

$$m_4 \cdot (\dot{v}_{y4} + w_{z4} \cdot v_{x4}) = F_{y41} + F_{y42} + F_{y43} + P_{y32} \tag{2.23}$$

$$I_{z4} \cdot \dot{w}_{z4} = P_{y32} \cdot l_{f4} - (dr_{41} \cdot F_{y41} + dr_{42} \cdot F_{y42} + dr_{43} \cdot F_{y43}) \tag{2.24}$$

There are certain simplifications made to the model as well.

- The vertical forces on the rear axle groups of all the units are assumed to be equal because usually the inter axle distance is very less, and the forces do not differ very much. Furthermore, the forces can be made equal by adjusting the air suspension in a real vehicle.
- Although modeling the suspension system could yield different and more realistic results. To limit the domain of work, it is assumed that the system is vertically rigid.
- The air drag acting on the vehicle, acts only on the tractor, only in the local x-direction. This implies that we do not take into consideration the effect of air drag on the sides of the vehicle units while the yaw angle of the units changes.

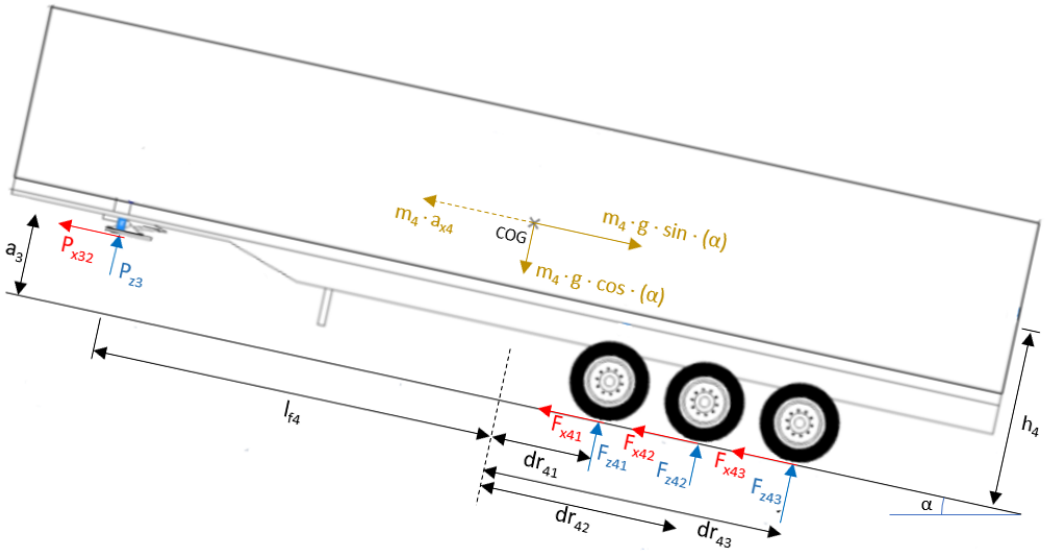

Figure 2.6: Diagram of Semi-trailer 2

Table 2.5: Vehicle parameters for the second semi-trailer

Parameter	Description	Length [m]
a_3	Height of the third coupling point from the ground surface	1.2
h_4	height of the cog	2.5
dr_{41}	distance of the 1st axle from the cog	1.16
dr_{42}	distance of the 2nd axle from the cog	2.47
dr_{43}	distance of the 3rd axle from the cog	3.78
lf_4	Distance of the cog from the third coupling point	6.32

Table 2.6

- The vehicle longitudinal speed is non zero. The tire model is not suitable for speeds approaching zero.
- The roll dynamics of the vehicle has been neglected.

2.3 Load Cases

In HCTs, the gross weight of the vehicle combination is mainly affected by the payload. The vehicle behavior is dictated by the position of the cog along the vehicle travel direction, and inertia. Hence to have a better understanding of the dynamics of the vehicle combination, the simulations are performed for three different situations of payload. These are at minimum, partial, and maximum payload. The kerb weight of each of the semi-trailers is assumed to be 5 tonnes. In the scenario of maximum payload, the gross weight of each of them is assumed to be 32.5 tonnes. In the case of partial payload, each semi-trailer weighs 18.75 tonnes. In all the test cases the semi-trailers are loaded equally. The different payloads lead to different

vertical forces available at the tires and the coupling points. To calculate forces for the axles of the tractor, the equations of vertical force and pitch equilibrium are:-

$$F_{z11} + F_{z12} + F_{z13} = m_1 \cdot g \cdot cos(\alpha) + P_{z1} \tag{2.25}$$

$$\begin{aligned} P_{x1} \cdot a_1 + F_{z12} \cdot (l_{r1} - dr_{12}) + F_{z13} \cdot (l_{r1} + dr_{13}) \\ = P_{z1} \cdot (l_{c12} - l_{f1}) + F_{z11} \cdot l_{f1} + h_1 \cdot (m_1 \cdot g \cdot sin(\alpha) + F_{air}) \end{aligned} \tag{2.26}$$

The equations for estimating the vertical force at first semi-trailer's axles:-

$$F_{z21} + F_{z22} + F_{z23} + P_{z1} = m_2 \cdot g \cdot cos(\alpha) + P_{z2} \tag{2.27}$$

$$\begin{aligned} P_{x21} \cdot a_2 + P_{z2} \cdot l_{c23} + F_{z21} \cdot dr_{21} + F_{z22} \cdot dr_{22} + F_{z23} \cdot dr_{23} \\ = P_{z1} \cdot l_{f2} + P_{x12} \cdot a_1 + m_2 \cdot g \cdot sin(\alpha) \cdot h_2 \end{aligned} \tag{2.28}$$

The equations for estimating the vertical force at the axles of e-dolly:-

$$F_{z31} + F_{z32} + P_{z2} = m_3 \cdot g \cdot cos(\alpha) + P_{z3} \tag{2.29}$$

$$\begin{aligned} P_{z2} \cdot l_{c23} + m_3 \cdot g \cdot sin(\alpha) \cdot h_3 + F_{z31} \cdot dr_{31} + P_{z3} \cdot l_{c34} \\ = F_{z32} \cdot dr_{32} + P_{x31} \cdot a_3 + P_{x22} \cdot a_2 \end{aligned} \tag{2.30}$$

The equations for estimating the vertical force at second semi-trailer's axles:-

$$F_{z41} + F_{z42} + F_{z43} + P_{z3} = m_4 \cdot g \cdot cos(\alpha) \tag{2.31}$$

$$\begin{aligned} F_{z41} \cdot dr_{41} + F_{z42} \cdot dr_{42} + F_{z43} \cdot dr_{43} \\ = P_{z3} \cdot l_{f4} + P_{x32} \cdot a_3 + m_4 \cdot g \cdot sin(\alpha) \end{aligned} \tag{2.32}$$

The individual axle vertical forces for each of the grouped axles of the vehicle are assumed to be divided equally among the axles of the respective axle group of the respective vehicle unit. As mentioned in the previous chapter, there are 4 maneuvers that are analyzed in this project, namely, Single Lane Change, Deceleration in a curve, and the maneuver to maintain a constant speed against a slope to estimate the Startability and Gradability. Although most of the input parameters like chassis dimensions, tire parameters, coefficients of friction, rolling resistance, aerodynamic drag, etc. stay the same, still there are some parameters that are changed for different simulations like steer angle, speed, mass, and grade percentage. The test cases have been modeled for situations of varying payload, vehicle speed, and road grade angle. The 4 test cases can be described here.

2.4 Test cases

2.4.1 Traction

The tests that fall under Traction, examine the vehicle's ability to, either maintain traction against a grade resistance or, accelerate from a standstill at zero grade, over a distance of 100 meters, to achieve the maximum possible speed. Although, the results largely depend on the size of the powertrain of the vehicle, but are also affected by payload distribution and powertrain layout. The performance parameter for Traction tests is either the road grade percentage (for judging Startability and Gradability) or it is the top speed (for Acceleration capability). To limit the scope of the thesis, the investigation has been done only for Startability and Gradability.

2.4.1.1 Startability

The maximum grade at which a vehicle can start and maintain a constant speed gives the startablity grade for that vehicle. However, since the implemented tire model can not be used for vehicle speeds that are very close to zero, the simulations of this model terminate at zero speeds. The simplification made is that the vehicle initial speed is around 0.1 km/h. Most of the parameters for gradability stay the same except for the constant vehicle speed. For gradability, the simulations are performed at a constant speed of 70 km/h.

2.4.1.2 Gradability

Gradability is defined as the maximum grade at which the vehicle can maintain a constant longitudinal speed of around 70 km/h. At such speeds, the aerodynamic drag cannot be neglected.

2.4.2 High Speed Stability

The performance tests that form the group of Stability tests is the Single Lane Change (SLC) maneuver. In an SLC maneuver, the tractor is subjected to a sine steer input, which leads to some lateral force at the tires, and yaw motion. It also generates some lateral force at the coupling point of the tractor-semitrailer. This force is responsible for the yaw motion of the semi-trailer. This effect continues on, as the yaw motion of the semi-trailer does the same for the dolly, and eventually the second semi-trailer. The units react successively to the steering actuation. It can be noticed that the yaw motion gets more amplified in terms of the magnitude of yaw velocity for the subsequent units.

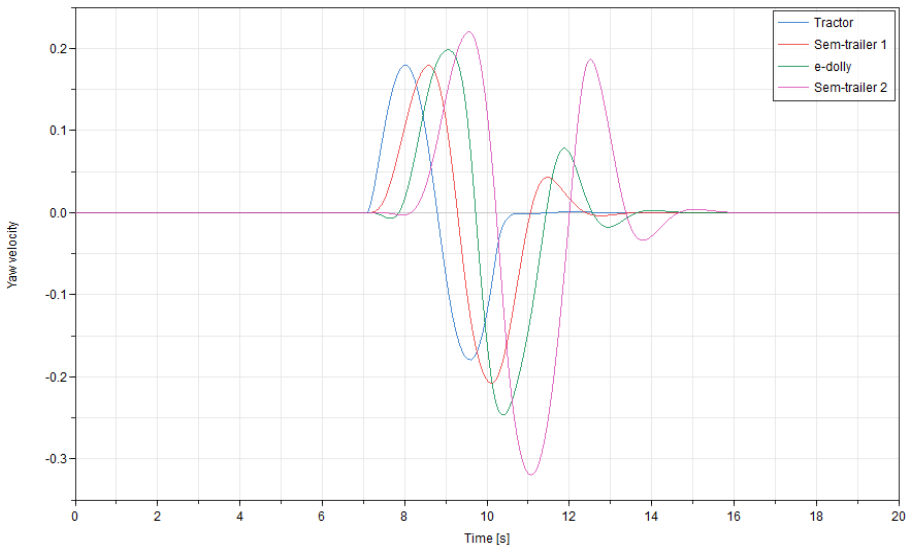

Figure 2.7: Yaw velocities vs Time for all four units

2.4.2.1 Rearward Amplification

The amplification of the yaw velocity is often studied as a parameter to have an understanding of the stability of the HCT vehicle at high speeds. The performance parameter is Rearward Amplification. It is the ratio of yaw velocity or lateral acceleration of the worst excited unit to the respective parameter of the least excited unit, which is the tractor. In this thesis work, the yaw velocity is used to compute RA. Hence the mathematical formula of RA can be written as:-

$$RA = \frac{max\_time(|\omega_4|)}{max\_time(|\omega_1|)} \tag{2.33}$$

As mentioned in the model assumptions, the vehicle model lacks the roll degree of freedom. In an actual HCT vehicle combination, there is lateral load transfer, hence there is a risk of rolling over at lateral accelerations of around 0.3g. So, to ensure the validity of the simulation results, the simulation collapses when the system reaches the acceleration of 3 m/s^2. The test cases are also modified to avoid high lateral acceleration on the vehicle units.

2.4.3 Deceleration

2.4.3.1 PBS approach

The test of Braking stability in a turn is performed to have an idea about the directional stability of the vehicle while decelerating in a turn. The PBS maneuver is to first maintain a constant radius of curvature and speed. Once it is reached, the vehicle is subjected to a constant deceleration. The measure that is used to study, is the maximum deceleration, which causes instability like jack-knife or trailer swing out.

2.4.3.2 Used approach

In this investigation, we have electric propulsion, which can be used for regenerative braking. From the perspective of energy efficiency, regenerative braking is more efficient, than the usual friction braking. However, too much regeneration can cause instability. Hence to capture the effects of regeneration on the vehicle's braking stability, the maneuver has been simulated for two cases. The first in one which, the deceleration is done via all-wheel friction braking. This is used as a reference case. The second case is when the model is subjected to the same driving conditions but it is decelerated only via regenerative braking on the e-dolly axle. The required decelerating torque is distributed equally among all axles in the former case and is limited by the maximum sliding friction available for the respective axle ($\mu_{slip} \cdot F_z$). However, in the latter case, it is applied only to the second axle of the e-dolly, and limited by the motor capacity. The stability of the vehicle is judged from the articulation angles, the maximum friction usage at the e-dolly axle (f_{max}), and the deceleration achieved, for both cases of braking.

2.4.3.3 Maneuver model

The simulation starts from high-speed steady-state cornering, which is assumed here to be at 80 km/h. To achieve that a step steer input is applied, and the vehicle takes a few seconds to reach the steady state. After that, it is subjected to the required deceleration. The vehicle undergoes sudden changes in the articulation angles and lateral acceleration. To check for jack-knifing and trailer swing out, there is a threshold value for articulation angles assumed to be 45 degrees. If the maxima of any articulation angle reaches that threshold, then the simulation collapses and that vehicle configuration can be considered unstable for those driving conditions. The simulation continues until it collapses or the vehicle comes to a halt.
To do a good investigation, the simulations have been carried out for different lateral accelerations and deceleration rates, on surfaces with different friction coefficients. Since the vehicle is more prone to be unstable when it is subjected to strong accelerations, therefore, to check for instability, and understand the difference between the two cases of deceleration mentioned above, the results are discussed for tight radius of curvatures, in the next chapter.

3
Results

3.1 Traction

The results of the tests performed for analyzing the Traction capability of the vehicle are shown via bar charts, and tables.

3.1.1 Startability

It is easy to guess that having an electric propulsion in the dolly will increase the startability of the vehicle. It can be judged very easily that the max inclination angle of the vehicle increases with decreasing payload, and having more propulsion power in the dolly.

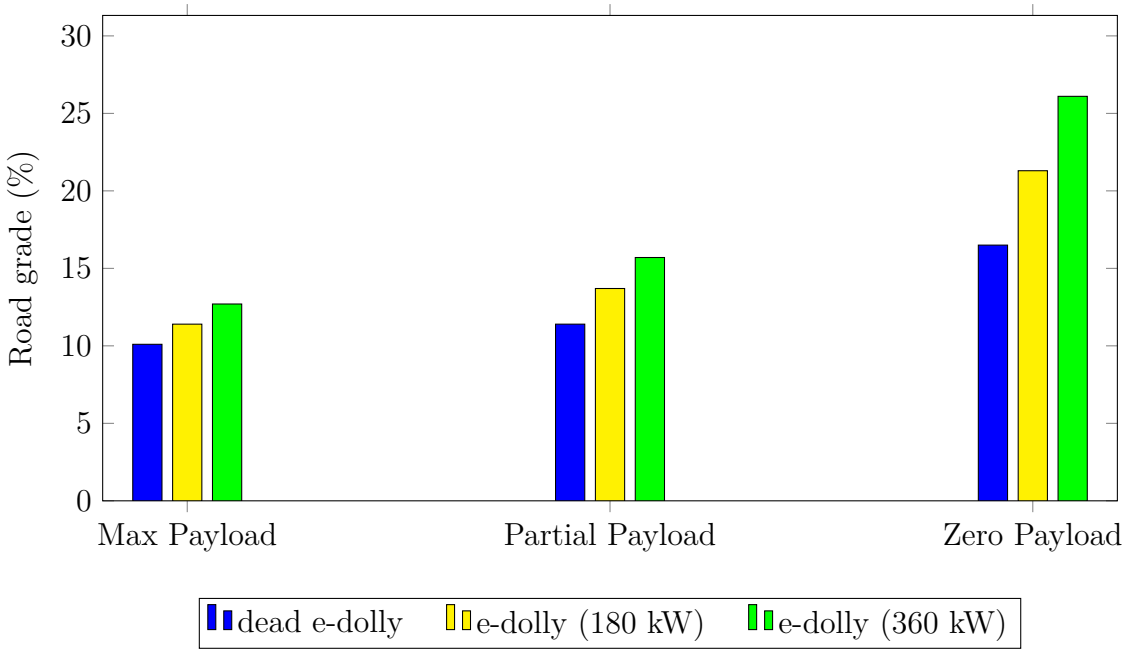

Figure 3.1: Startability results

The results show that the performance is affected more severely with decreasing payload. At a high payload, the tractor is able to generate more propulsion torque than the e-dolly. This can be justified by the fact that the decreased vertical forces on the tires limit the longitudinal force that can be generated by the tractor for the same longitudinal slip. However, the decreased payload does not have the same

effect on the dolly, so it can be operated at maximum power. Hence, the dolly adds more to the overall performance. This is also supported by the fact that having higher dolly power at lower payloads shows much better results than doing the same with high payload operations.

3.1.2 Gradability

The results show that at such high-speed operations, since torque supplied by the motor is decreased, there is less increment to the maximum grade angle. As we move ahead, and simulate for the scenarios of partial and zero payload, it is clearly visible, that as we decrease the load, the climbing angle increases.

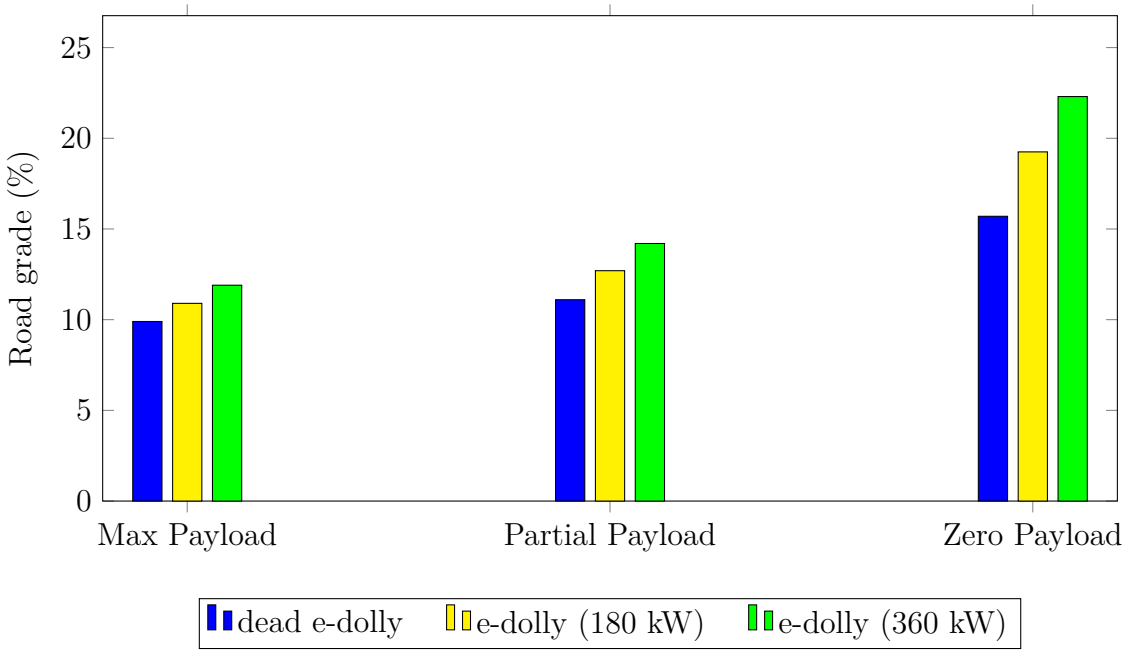

Figure 3.2: Gradability results

PBS Measure	Road Grade (%)	Without e-Dolly	With e-Dolly (180 Kw)	With e-Dolly (360 Kw)
Startability	Empty	16.5	21.3	26.1
	Partial Payload	11.4	13.7	15.7
	Max Payload	10.1	11.4	12.7
Gradability	Empty	15.7	19.25	22.3
	Partial Payload	11.1	12.7	14.2
	Max Payload	9.9	10.9	11.9

Table 3.1: Results of Startability and Gradability

Henceforth, the implementation of the e-dolly improves the Traction capability of the A-double combination vehicle. Since, the Traction capacity of the vehicle improves with an e-dolly, in all the test cases, it becomes pretty easy to judge that it will improve even for the surfaces with lower friction coefficients. Although the

percentage by which it does, may vary, it becomes a little bit less motivating to investigate the same model for low friction surfaces for Traction capability. In other words, the tests conducted for high friction surface is enough to conclude that using an e-dolly will for sure prove to be better than a conventional A-double, and there is not any unpredictable situation for that.

3.2 Stability

The results of the tests performed for analyzing the Stability are shown via tables and graphs.

3.2.1 Single Lane Change maneuver

Rearward Amplification	Dead e-Dolly	e-Dolly (180 Kw)	e-Dolly (360 Kw)
Empty	1.638	1.73	1.813
Partial Payload	1.55	1.568	1.568
Max Payload	1.537	1.544	1.545

Table 3.2: Results of Single Lane Change for dry ashphalt

The results imply that RWA decreases significantly with increasing payload, and increases, with increasing e-dolly power. However since it is a high friction case, the vehicle does not lose traction. With increasing payload, the effect of having an e-dolly is not that highlighting because the vertical forces increase and make the tires less prone to getting saturated. For the same reason, the influence is more clearly visible in the low-friction test case.

Rearward Amplification	Dead e-Dolly	e-Dolly (180 Kw)	e-Dolly (360 Kw)
Empty	1.934	NaN	NaN
Partial Payload	1.812	1.875	NaN
Max Payload	1.779	1.824	1.869

Table 3.3: Results of Single Lane Change for wet asphalt

In the table above, NaN indicates the occurrence of Jack-Knifing. In the test case with empty payload, on a wet asphalt road, the effect of e-dolly makes the combination unstable and causes the rear trailer to swing out.

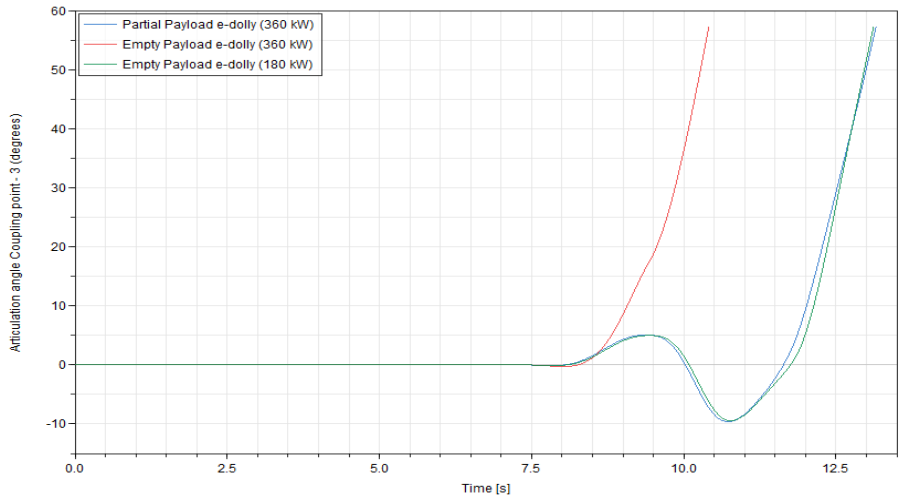

Figure 3.3: Articulation angle vs Time for the three failed cases of SLC

The case of partial payload, with 360 kW of electric power gives the same result. As mentioned earlier, the simulation is terminated when the articulation angle reaches a certain threshold. It can be explained that as the inertia increases, the axle vertical forces increase, and the vehicle units exhibit lesser excitation for the same amount of lateral and longitudinal forces. Hence the response in terms of yaw velocity, at empty payload, is the strongest. The presence of e-dolly causes greater variation in the hinge forces during the maneuver, which leads to higher tire forces and the tires of the trailing units become more prone to the loss of traction.

3.2.2 Decelerating in a curve

The test case of deceleration in a curve has been explained in the previous chapter. In this section, the results are explained for the cases with highest deceleration of 1 m/s^2 and lateral acceleration of 3 m/s^2.

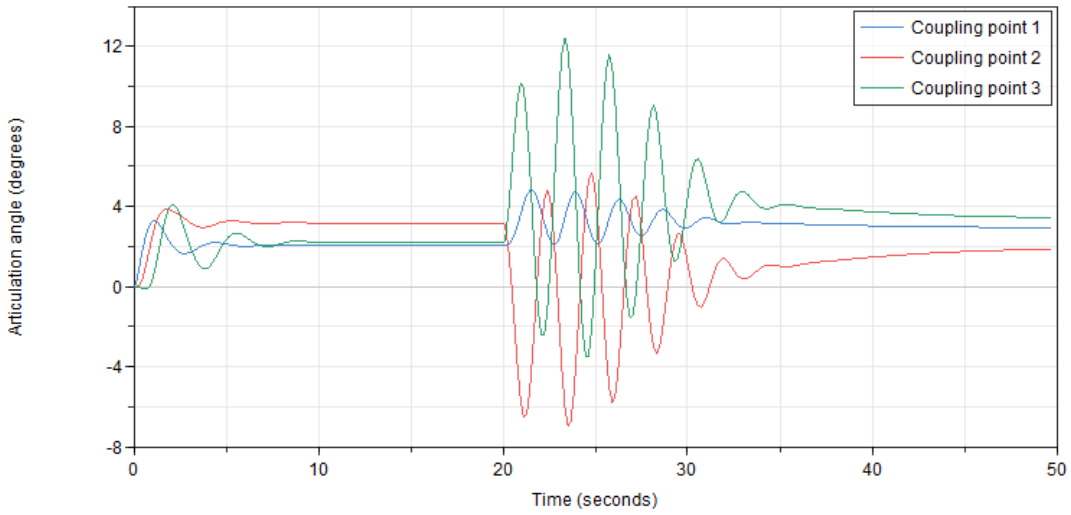

Figure 3.4: Articulation angle vs Time

The reason that the retardation is kept so low is because the dolly which is braking the vehicle model with regeneration, is limited by the maximum torque that the motor can apply to the axles for regenerating. Hence to make a comparison there are three cases of payload, simulated for the maneuver, with 3 cases of decelerating. One of them is the friction braking on all axles. The other two have e-dollies of 180 kW and 360 kW respectively.

The figure above shows the variation of articulation angles of the vehicle combination with e-dolly regeneration braking on wet asphalt with $\mu_{peak} = 0.43$, with both semi-trailers being empty. The result imply that as the vehicle undergoes deceleration, because of the low friction, the tires of the second semi-trailer use almost all of the friction, and the tires of the driven axle of the e-dolly get saturated soon, and consequently the dolly axle loses traction. The inertia behind the e-dolly (empty semi-trailer 2) pushes it to swing out, because the driven axle of the dolly cannot take any lateral force. This leads to a temporary drop in the deceleration of the vehicle units ahead, as the driven axle cannot generate the same deceleration, while it is slipping out. The units ahead of the e-dolly, which were earlier being pulled behind by the e-dolly are no longer undergoing the same deceleration and provide a temporary pulling motion to the dolly, that stretches it, and the e-dolly is started to be pulled straight, towards zero articulation angle (of the coupling point 3). The axle of the e-dolly again starts to decelerate more, and loses traction again for the same reason as stated above. This time it swings in the opposite direction. And again it returns back due to stretching by the units in the front. This oscillatory motion and the phase difference in the deceleration of the individual units continues till the vehicle speed decreases to certain extent, that significantly lowers the lateral acceleration on the remaining tires of the units, and allows them to track the dolly along, even if the tires of its driven axle are slipping.

Since the dolly can lose traction in some cases, so to study the stability better, the fraction of friction used up at the driven axle of the dolly has been calculated as well. The variation with time is shown in the following figure.

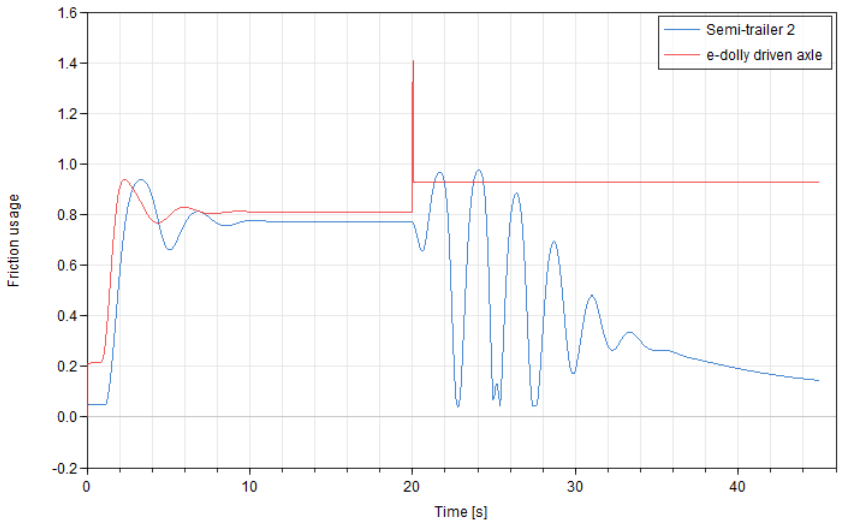

Figure 3.5: Fraction of friction used vs Time

It is calculated by the formula,

$$f = \frac{\sqrt{F_x^2 + F_y^2}}{\mu_{peak} \cdot F_z} \tag{3.1}$$

It can be noticed that the friction usage of the tires of the driving axle of the e-dolly, in this case reaches its sliding force limit. In the formula, $\mu_{peak} > \mu_{slip}$, hence even if the tires are saturated, the fraction of friction used is seen as less than 1 ($F_{xy} = \mu_{slip} \cdot F_z$). Lastly, as the e-dolly is limited by the retarding torque, hence a fair parameter to make the comparison is the deceleration of the tractor unit, which has been computed for each of the test cases.
The corresponding results of variation of articulation angles for the all axle axle friction braking case for the same system parameters is :-

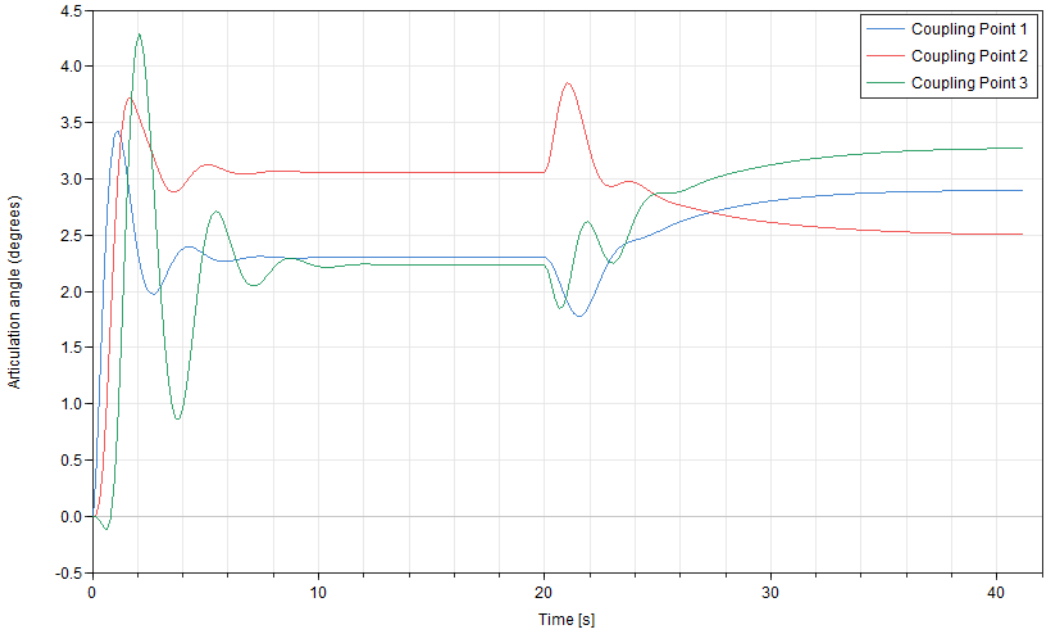

Figure 3.6: Articulation angle vs Time for all axle friction braking

It can be noticed that since all the axles brake the vehicle, therefore the vehicle is stable and there is a very little change in the articulation angles.

Table 3.4: Performance parameters at different load and braking scenario for wet asphalt

Maximum Articulation	Friction Brake			e-dolly (180 kW)			e-dolly (360 kW)		
	θ_{max}	f_{max}	$\dot{v}_x$	θ_{max}	f_{max}	$\dot{v}_x$	θ_{max}	f_{max}	$\dot{v}_x$
No Load	3.84	0.78	1	3.6	0.93	0.7	12.6	0.93	0.68
Partial Load	3.84	0.84	1	3.5	0.93	0.44	8.8	0.93	0.56
Max Load	4.36	0.91	1	3.6	0.9	0.36	3.5	1	0.51

The results imply that, for surfaces with low friction, with increasing payload, the friction usage of the e-dolly axle decreases, and it becomes more stable. However,

the deceleration decreases. Hence, it could be challenging to use a high-power e-dolly on low-friction surfaces, because it is more prone to slide and lose traction. However, for super high payload situations, it could be safe to put it in use.

Table 3.5: Performance parameters at different load and braking scenario for dry asphalt

Maximum Articulation	Friction Brake			e-dolly (180 kW)			e-dolly (360 kW)		
	θ_{max}	f_{max}	$\dot{v}_x$	θ_{max}	f_{max}	$\dot{v}_x$	θ_{max}	f_{max}	$\dot{v}_x$
No Load	3.3	0.4	1	2.7	0.57	0.7	2.8	0.9	1
Partial Load	3.75	0.43	1	3.24	0.5	0.44	3	0.7	0.68
Max Load	4.5	0.5	1	3.8	0.5	0.37	3.56	0.57	0.52

The results from the maneuvers simulated for dry asphalt imply that applying regenerative braking with an e-dolly is safe and the vehicle is less likely to lose stability. The maximum articulation angle at any coupling point tends to decrease as the dolly power increases. It could be explained as, the friction coefficient is high, all of the motor torque is used up, without the loss of traction, hence the possibility of swing out is less. The deceleration with 360 kW e-dolly can compete with friction braking in terms of deceleration, but only at the empty payload.

As the payload increases the maximum articulation angle increases because of the heavy mass that follows the e-dolly. But it is higher for friction braking than for regenerative braking because of the pulling effect that the vehicle goes through when decelerating only on the dolly axle. Hence using a high capacity e-dolly in high friction surfaces is more suitable from an efficiency and safety point of view.

4
Conclusion

The central idea behind the thesis work is to analyze the vehicle dynamics of an A-double combination with an electrified dolly, on the basis of tests mentioned in the PBS framework. After a brief literature review of the existing PBS framework, the feasibility of some tools to create a vehicle model, like IPG TruckMaker, and Dymola, was compared. The vehicle model created for this investigation contains a lot of simplifications to avoid complexity. However, the models of the vehicle and test cases, are very clear and understandable and yet sufficient to capture some differences between the vehicle behavior of a conventional A-double vs. an A-double with an e-dolly. The results show that using an e-dolly to minimize environmental impact, to carry heavier payloads could be a potential trade-off between Safety and Performance.

The simulations of the Traction suggest that the combination with e-dolly will perform better than a conventional one, particularly for low payload situations. Whereas, the study done with the tests of high-speed stability shows that there are some cases when the electrified A-double could cause a risk of creating dangerous situations. For example, the Jack-knifing that happens in a Single Lane Change maneuver for low payloads. For the simulation of Deceleration in a Curve in high friction surfaces, the e-dolly proves to be a little bit more stable than all-wheel braking, for high payload situations on high friction surfaces. However, the oscillatory yaw motion is also observed when braking via a high-powered e-dolly on low friction. This motivates the need for controllers to control the torque distribution for the e-dolly.

This suggests that the current PBS framework is not enough to ensure the safe operation of HCT combinations with an electrified dolly. There is a need to create test maneuvers and additional performance measures to study the vehicle behavior for High-speed stability and Deceleration in curve, which could involve the usage of controllers to control certain aspects like wheel slip, torque distribution among the powered axles (both tractor and e-dolly).

4.1 Future Work

The work that has been concluded above, gives a lot of scope to carry out more work in the domain of PBS for electrified HCT combinations in the future.

- The study of High-speed and Braking stability using a PBS approach with optimal torque distribution among the tractor and the e-dolly.
- To study the braking stability in a curve better, the simulations can also be carried out for the case of engine braking (assuming that there is a Diesel or electrically propelled tractor), and the results can be compared with all-wheel friction braking and the e-dolly regenerative braking.
- A double-track model vehicle can be created to give more realistic results, and study, the effect of lateral load transfer, and the torque between the left and right side through an axle differential.
- The dynamics can also be analyzed for the surface with varying friction, and/or for the situations of having different surface friction on the two wheels of the same axle.
- The study of the maneuvers that are simulated in this work can be extended to have a non-zero grade resistance, to understand the vehicle behavior for different road surface inclinations.
- The study of A-double with an electrified semi-trailer can also be done, using a PBS approach, and can be compared with the e-dolly case, on the basis of safety.

Bibliography

[1] Volvo. (2023). Volvo FH Electric Specifications. https://www.volvotrucks.com/en-en/trucks/trucks/volvo-fh/volvo-fh-electric.html

[2] Kharazzi, S. (2017). Peformance based standards for high capacity transports in Sweden.

[3] CLOSER (2017). Roadmap HCT Road.

[4] Kharazzi, S. (2018). Peformance based standards project in Sweden.

[5] Volvo Trucks.(2023).FH16 6X4 Tractor - Rear Air Suspension N3G:Truck Data-sheet[Data-sheet].Volvo Trucks. https://stpi.it.volvo.com/STPIFiles/Volvo/ModelRange/fh64t6a_gbr_eng.pdf

[6] Dalemo, A., Djerf, E., Hägglund, A., Poveda, D., Ramsberg, J., (2023). A model of REVERE A-double with e-dolly.

[7] Jacobson, B., Sundström, P., Kharazzi, S., Fröjd, N., Islam, M., (2017). An Open Assessment Tool for Performance Based Standards of Long Combination Vehicles.

[8] Jacobson, B., Jonasson, M., Bruzelius, F. (2022) Compendium in Vehicle Motion Engineering. Chalmers University of Technology.

A

Appendix 1

This section consists of the model of the vehicle and the test case for the simulation of Deceleration in a curve. For the sake of brevity, the code for the maneuvers of High Speed Stability and Traction capability have note been shared.

```
model Deceleration_in_a_curve
parameter Modelica.Units.SI.Mass m11 = 5270 "Equivalent mass on 1st
    axle of tractor";
parameter Modelica.Units.SI.Mass m12 = 3760 "Equivalent mass on 2nd
    axle of tractor";
parameter Modelica.Units.SI.Mass m2 = 5000 "Mass of trailer-1";
parameter Modelica.Units.SI.Mass m3 = 5000 "Mass of electrified dolly
    ";
parameter Modelica.Units.SI.Mass m4 = 5000 "Mass of trailer-2";

parameter Modelica.Units.SI.Inertia i1 = 25000 "Yaw nertia of tractor
    ";
parameter Modelica.Units.SI.Inertia i3 = 7000 "Yaw nertia of dolly";

parameter Modelica.Units.SI.Angle slope = 0 "Road inclination angle";
parameter Modelica.Units.SI.Power P_em_max = 360000 "Max power of the
    motor"; // Can be changed to 180000 as well.

parameter Modelica.Units.SI.Inertia Jwh = 10 "Inertia of one wheel";
parameter Modelica.Units.SI.Length r = 0.5 "Wheel radius";
parameter Modelica.Units.SI.Area A_f = 10 "Frontal area of the tractor
    ";
parameter Modelica.Units.SI.Density rho = 1.23 "Density of air";
parameter Modelica.Units.SI.DimensionlessRatio cd = 0.8 "Aerodynamic
    drag coefficient of the tractor";

parameter Modelica.Units.SI.DimensionlessRatio CCy = 7.5 "Lateral slip
     stifness coefficient";

parameter Modelica.Units.SI.DimensionlessRatio rrc = 0.01 "Rolling
    resistance coefficient";
parameter Modelica.Units.SI.DimensionlessRatio mu_sl=0.8
   "Slip friciton coefficient";
 parameter Modelica.Units.SI.DimensionlessRatio mu_st=1.0
   "Stic friciton coefficient";

parameter Modelica.Units.SI.Acceleration g = 9.81 "Accleration due to
    gravity";
```

```
parameter Modelica.Units.SI.Length wb = 4.085 "Theoretical wheelbase
   of tractor";
parameter Modelica.Units.SI.Length l1c = 3.45 "Distance of the first
   coupling point from front axle of tractor";
parameter Modelica.Units.SI.Length tw = 2 "Track width of all units";

parameter Modelica.Units.SI.Length lf2 = 6.320 "cog(trailer-1) to
   articulation point of tractor-trailer";
parameter Modelica.Units.SI.Length lr2 = 2.470 "cog to center axle of
   trailer-1";
parameter Modelica.Units.SI.Length dr21 = 1.160 "cog to first axle of
   tractor";
parameter Modelica.Units.SI.Length dr22 = 2.470 "cog to second axle of
    tractor";
parameter Modelica.Units.SI.Length dr23 = 3.780 "cog to third axle of
   tractor";
parameter Modelica.Units.SI.Length la22c = 4.780 "second articulation
   point of trailer-1 to cg of trailer-1 (theoretical)";

parameter Modelica.Units.SI.Length lac32 = 4.360 "articulation point
   of trailer1-dolly to cg of e-dolly ";
parameter Modelica.Units.SI.Length lac34 = 0.080 "cog (dolly) to
   articulation point of trailer2-dolly";
parameter Modelica.Units.SI.Length dr31 = 0.660 "cog to first axle of
   e-dolly";
parameter Modelica.Units.SI.Length dr32 = 0.660 "cog to second axle of
    e-dolly";

parameter Modelica.Units.SI.Length lf4 = 6.320 "cog(trailer-2) to
   articulation point of dolly-trailer-2";
parameter Modelica.Units.SI.Length lr4 = 2.470 "cog to center axle of
   trailer-2";
parameter Modelica.Units.SI.Length dr41 = 1.160 "cog to first axle of
   trailer";
parameter Modelica.Units.SI.Length dr42 = 2.470 "cog to second axle of
    trailer";
parameter Modelica.Units.SI.Length dr43 = 3.780 "cog to third axle of
   trailer";

parameter Modelica.Units.SI.Length h1 = 1.2 "cog height tractor(from
   ground surface)";
parameter Modelica.Units.SI.Length h2 = 2.5 "cog height trailer-1 (
   from ground surface)";
parameter Modelica.Units.SI.Length h3 = 0.6 "cog height e-dolly (from
   ground surface)";
parameter Modelica.Units.SI.Length h4 = 2.5 "cog height trailer-1 (
   from ground surface)";
parameter Modelica.Units.SI.Length a1 = 1.0 "articulation point 1
   height trailer(from ground surface)";
parameter Modelica.Units.SI.Length a2 = 0.5 "distance between cog of
   trailer-1 and 2nd articulation point(from ground surface)";
parameter Modelica.Units.SI.Length a3 = 1.2 "articulation point 1
   height trailer(from ground surface)";

parameter Modelica.Units.SI.DimensionlessRatio g_em = 14.7 "Gear ratio
    of motor to dolly axle";
```

```
parameter Modelica.Units.SI.Acceleration aref = -1 "Demanded
    acceleration";
parameter Modelica.Units.SI.DimensionlessRatio brake_type = 3 "3
    stands for regen brake, 1 for all axle, 2 for engine";

Modelica.Units.SI.Velocity vx1, vy1, v1fxw, v1fyw, v11y, v12y, v13y,
    vx2, vy2, v21y, v22y, v23y, vx3, vy3, v31y, v32y;
Modelica.Units.SI.Velocity v11cy, v12cy, v22cy, v23cy, v33cy, v34cy;
    //Lateral speeds of the coupling points
Modelica.Units.SI.Velocity vx4, vy4, v41y, v42y, v43y;
Modelica.Units.SI.AngularVelocity wz1, wz2, wz3, wz4; //yaw velocities
     of the units
Modelica.Units.SI.AngularVelocity w13, w12, w32, w11, w21, w22, w23,
    w31, w41, w42, w43, w_em; //wheel rotational speeds
Modelica.Units.SI.Angle steer, theta_1, theta_2, theta_3, phi_1, phi_2
    , phi_3, phi_4;
Modelica.Units.SI.Force Fz11, Fz12, Fz13, Fz21, Fz22, Fz23, Fz31, Fz32
    , Fz41, Fz42, Fz43, Fz;
Modelica.Units.SI.Force P1z, P2z, P3z; // Hinge vertical forces;
Modelica.Units.SI.Force P1x, P2x(start=1), P2y, P1y, P3x, P3y, P4x,
    P4y, P5x, P5y, P6x, P6y; // Hinge lateral and longitudinal forces
Modelica.Units.SI.Force Fx11, Fx12, Fy11, Fy12, Fx13, Fy13, Fx21, Fx22
    , Fx23, Fy21, Fy22, Fy23, Fx31, Fx32, Fy31, Fy32, Fx41, Fx42, Fx43
    , Fy41, Fy42, Fy43, max_f32, max_f31, max_f43;
Modelica.Units.SI.DimensionlessRatio sy11, sy12, sy13, sy21, sy22,
    sy23, sy31, sy32, sy41, sy42, sy43;
Modelica.Units.SI.DimensionlessRatio sx11, sx12, sx13, sx21, sx22,
    sx23, sx31, sx32, sx41, sx42, sx43;
Modelica.Units.SI.DimensionlessRatio sk11, sk12, sk13, sk21, sk22,
    sk23, sk31, sk32, sk41, sk42, sk43;
Modelica.Units.SI.DimensionlessRatio s11, s12, s13, s21, s22, s23, s31
    , s32, s41, s42, s43;
Modelica.Units.SI.DimensionlessRatio o11, o12, o13, o21, o22, o23, o31
    , o32, o41, o42, o43;
Modelica.Units.SI.Length lf1, lr1;
Modelica.Units.SI.DimensionlessRatio RWA;
Modelica.Units.SI.Acceleration ay1, ay2, ay3, ay4 "Lateral accleration
     of units";
Modelica.Units.SI.Length R1, R2, R3, R4 "Radius of curvatures";
Modelica.Units.SI.Length x1, y1, x2, y2, x3, y3, x4, y4;
Modelica.Units.SI.DimensionlessRatio f, k, CCx, sk_threshold, fu32,
    fu31, fu43, mu_peak;
Modelica.Units.SI.Mass m1, m_gross;
Modelica.Units.SI.Torque Tr, T_em_max, T_em;
Modelica.Units.SI.Torque Tap11, Tap12, Tap13, Tap21, Tap22, Tap23,
    Tap31, Tap32, Tap41, Tap42, Tap43; //T_fec;
Boolean dolly;

Modelica.Units.SI.AngularVelocity peak_first(start=0); // peak1(start
    =0), peak2(start=0);
Modelica.Units.SI.AngularVelocity peak_last(start=0);
Modelica.Units.SI.Length hsso "High speed steady state off-tracking";
Modelica.Units.SI.DimensionlessRatio nb "Number of friction braked
    axles";
Modelica.Units.SI.Inertia i2, i4;
Real flag_vel(start=0), flag_theta(start=0);
```

```
 //Real flag_ay(start=0);

 Modelica.Units.SI.Acceleration ax;
 import Modelica.Constants.pi;

// parameter Real steer[73233,1] = DataFiles.readMATmatrix("
    random_steering.mat", "steer_random");

initial equation
 w12 = vx1/r;
 w13 = vx1/r;
 w11 = vx1/r;

 w21 = vx2/r;
 w22 = vx2/r;
 w23 = vx2/r;

 w31 = vx3/r;
 w32 = vx3/r;

 w41 = vx4/r;
 w42 = vx4/r;
 w43 = vx4/r;

 vx1 = 80/3.6;
 vx2 = 80/3.6;
 vx3 = 80/3.6;
 vx4 = 80/3.6;

equation
  mu_peak = mu_st*((4 - 3*(mu_sl/mu_st))/(3 - 2*(mu_sl/mu_st))^2) "
     Coefficient of peak friction";
  T_em_max = P_em_max*0.0010123*7/3 "Max torque of the electric motor";

  Fz = Fz11 + Fz12 + Fz13 + Fz21 + Fz22 + Fz23 + Fz31 + Fz32 + Fz41 +
     Fz42 + Fz43;
  m_gross = m1 + m2 + m3 + m4;

  dolly = if brake_type == 1 then false else true;

  Tr = r*((m_gross + 26*Jwh/(r^2))*ax + 0.5*rho*A_f*cd*vx1^2 + m_gross*
     g*sin(slope)) + rrc*Fz*sign(vx1);

  ax = if time < 20 then 0.14 else aref;
  //ax = if regen_brk == true then (if time < 10 then 0 else sign(aref)
     *min(abs(aref),abs(T_em*g_em/m_gross*r))) else (if time < 10 then
      0 else sign(aref)*min(abs(aref),abs(0.5*mu_sl*Fz/m_gross)));

  w_em = w32*g_em;
  T_em = if dolly == true then sign(ax)*(if w_em < P_em_max/T_em_max
     then T_em_max else P_em_max/w_em) else 0;

  steer = 0.027;

    ////////////////////   ALL AXLE BRAKING   ////////////////////
```

```
if brake_type == 1 then
  nb = 11;
  Tap11 = if ax>=0 then 0 else sign(ax)*min(mu_sl*Fz11*r,abs(Tr/nb));
  Tap12 = if ax>=0 then Tr/2 else sign(ax)*min(mu_sl*Fz12*r,abs(Tr/nb
     ));
  Tap13 = if ax>=0 then Tr/2 else sign(ax)*min(mu_sl*Fz13*r,abs(Tr/nb
     ));
  Tap21 = if ax>=0 then 0 else sign(ax)*min(mu_sl*Fz21*r,abs(Tr/nb));
  Tap22 = if ax>=0 then 0 else sign(ax)*min(mu_sl*Fz22*r,abs(Tr/nb));
  Tap23 = if ax>=0 then 0 else sign(ax)*min(mu_sl*Fz23*r,abs(Tr/nb));
  Tap31 = if ax>=0 then 0 else sign(ax)*min(mu_sl*Fz31*r,abs(Tr/nb));
  Tap32 = if ax>=0 then 0 else sign(ax)*min(mu_sl*Fz32*r,abs(Tr/nb));
  // if aref is negative then T_em is negative
  Tap41 = if ax>=0 then 0 else sign(ax)*min(mu_sl*Fz41*r,abs(Tr/nb));
  Tap42 = if ax>=0 then 0 else sign(ax)*min(mu_sl*Fz42*r,abs(Tr/nb));
  Tap43 = if ax>=0 then 0 else sign(ax)*min(mu_sl*Fz43*r,abs(Tr/nb));

  ////////////////////  ENGINE BRAKING  ///////////////////////

elseif brake_type == 2 then
  nb = 2;
  Tap11 = 0;
  Tap12 = if ax>=0 then (Tr - Tap32)/2 else sign(Tr)*min(mu_sl*Fz12*r
     ,abs(Tr/nb));
  Tap13 = if ax>=0 then (Tr - Tap32)/2 else sign(Tr)*min(mu_sl*Fz13*r
     ,abs(Tr/nb));
  Tap21 = 0;
  Tap22 = 0;
  Tap23 = 0;
  Tap31 = 0;
  Tap32 = if ax>=0 then (if dolly == true then min(T_em*g_em,Tr/3)
     else 0) else 0;
  // if aref is negative then T_em is negative
  Tap41 = 0;
  Tap42 = 0;
  Tap43 = 0;

  ////////////////// REGEN BRAKING ON THE 2ND AXLE OF THE E-DOLLY
     /////////////////
else
  nb = 1;
  Tap11 = 0;
  Tap12 = if ax>=0 then (Tr - Tap32)/2 else 0;
  Tap13 = if ax>=0 then (Tr - Tap32)/2 else 0;
  Tap21 = 0;
  Tap22 = 0;
  Tap23 = 0;
  Tap31 = 0;
  Tap32 = if ax>=0 then min(T_em*g_em,Tr/3) else sign(ax)*min(abs(
     T_em*g_em),abs(Tr));
  // if aref is negative then T_em is negative
  Tap41 = 0;
  Tap42 = 0;
  Tap43 = 0;
end if;
```

```
  when vx1 <= 0.0001 then
    flag_vel = 1;
terminate("Zero velocity situation reached");
  end when;


  when abs(theta_1) > 0.75 or abs(theta_2) > 0.75 or abs(theta_3) >
     0.75 then
    flag_theta = 1;
terminate("Jack-knifing situation reached");
  end when;

i2 = m2*((1.5 + lf2 + la22c + 1)^2 + tw^2)/12 "Yaw inertia of first
   semi-trailer";
i4 = m4*((1.5 + lf2 + la22c + 1)^2 + tw^2)/12 "Yaw inertia of first
   semi-trailer";

RWA = if peak_first > 0 then peak_last/peak_first else -1;

when (abs(wz1) > pre(peak_first) and der(abs(wz1)) < 0 and abs(wz1) >
    0.05) then
   peak_first = abs(wz1);
end when;

when (abs(wz3) > pre(peak_last) and der(abs(wz3)) < 0 and abs(wz3) >
   0.05) then
   peak_last = abs(wz3);
end when;

hsso = if steer <> 0 and (der(wz1) <= 0.005 and der(wz2) <= 0.001 and
    der(wz3) <= 0.001 and der(wz4) <= 0.001) then R4-R1 else 0 "High
    speed steady state off-tracking";

sk_threshold = 3*mu_st/CCy;
f = 1/pi "Frequency of steering input";
k =  1.65 "auxillary parameter(Ratio of longitudinal and lateral slip
    stiffness coefficients)";
CCx = k*CCy;

//---------Calculations for cog location of tractor----///////
m1 = m11+m12 "Total mass of the tractor";
m11*g*lf1 = m12*g*lr1 "Pitch equilibrium equation of tractor(Without
   the influence of trailer)";
lf1 + lr1 = wb;

Fz11 + Fz12 + Fz13 = m1*g*cos(slope) + P1z "Vertical force
   equilibrium of forst semi-trailer";
P1x*a1 + Fz12*(lr1 - 0.685) + Fz13*(lr1 + 0.685) = P1z*(l1c-lf1) +
   Fz11*lf1 + h1*(m1*g*sin(slope) + 0.5*rho*A_f*cd*vx1^2) "Pitch
   equilibrium equation of tractor(Without the influence of trailer)
   ";
Fz12 = Fz13;

Fz21 = Fz22;
Fz22 = Fz23;
```

```
 Fz21 + Fz22 + Fz23 + P1z = m2*g*cos(slope) + P2z;
 Fz21*dr21 + Fz22*dr22 + Fz23*dr23 + P2z*la22c + P3x*a2 = m2*g*sin(
    slope)*h2 + P2x*a1 + P1z*lf2;


 Fz41 + Fz42 + Fz43 + P3z = m4*g*cos(slope);
 Fz41*dr41 + Fz42*dr42 + Fz43*dr43 = m4*g*sin(slope)*h4 + P6x*a3 + P3z
    *lf4;

 Fz41 = Fz42;
 Fz42 = Fz43;

 Fz31 + Fz32 + P2z = m3*g*cos(slope) + P3z;
 Fz31*dr31 + P3z*lac34 + m3*g*sin(slope) + P2z*lac32 = Fz32*dr32 + P4x
    *a2 + P5x*a3;
 Fz31 = Fz32;


 //////////-----------------Equations of motion for tractor
    ------------------/////////////

m1*(der(vx1) - wz1*vy1) = (Fx11*cos(steer) - Fy11*sin(steer) + Fx12 +
    Fx13) + P1x - 0.5*rho*A_f*cd*vx1^2 - m1*g*sin(slope) "Longitudinal
     force equilibrium";
m1*(der(vy1) + wz1*vx1) = (Fx11*sin(steer) + Fy11*cos(steer) + Fy12 +
    Fy13) + P1y "Lateral force equilibrium";
i1*der(wz1) = (lf1*(Fx11*sin(steer) + Fy11*cos(steer)) - Fy12*(lr1 -
    0.685) - Fy13*(lr1 + 0.685)) - P1y*(l1c - lf1) "Yaw equilibrium";

ay1 = der(vy1) + wz1*vx1 "Lateral acceleration of the tractor";
R1 = if wz1 == 0 then 0 else abs(sqrt(vx1^2 + vy1^2))/wz1 "Radius of
    curvature"; //Valid for steady state cornering only

sy11 = v1fyw/abs(r*w11) "Lateral slip at the first axle";
sy12 = v12y/abs(r*w12) "Lateral slip at the second axle";
sy13 = v13y/abs(r*w13) "Lateral slip at the third axle";

o11 = 1 - ((sk11*CCy)/3*mu_st);
o12 = 1 - ((sk12*CCy)/3*mu_st);
o13 = 1 - ((sk13*CCy)/3*mu_st);

Tap11 = Jwh*der(w11) + Fx11*r + rrc*Fz11*sign(vx1) "Wheel torque
    equilibrium for first axle";
Fx11 = if (sk11 > sk_threshold or sign(w11*vx1) < 0) then mu_sl*Fz11*
    cos(atan2(-v1fyw,(r*w11 - v1fxw))) else Fz11*((CCx*sx11*o11^2) + (
    mu_sl*cos(atan2(-v1fyw,(r*w11 - v1fxw)))*(1-3*o11^2+2*o11^3)));
sx11 = (r*w11 - v1fxw)/abs(r*w11) "Longitudinal slip at the first axle
    ";

Tap12 = Jwh*der(w12) + Fx12*r + rrc*Fz12*sign(vx1) "Wheel torque
    equilibrium for second axle";
Fx12 = if (sk12 > sk_threshold or sign(w12*vx1) < 0) then mu_sl*Fz12*
    cos(atan2(-v12y,(r*w12 - vx1))) else Fz12*((CCx*sx12*o12^2) + (
    mu_sl*cos(atan2(-v12y,(r*w12 - vx1)))*(1-3*o12^2+2*o12^3)));
sx12 = (r*w12 - vx1)/abs(r*w12) "Longitudinal slip at the second axle
    ";
```

```
Tap13 = Jwh*der(w13) + Fx13*r + rrc*Fz13*sign(vx1) "Wheel torque
   equilibrium for third axle";
Fx13 = if (sk13 > sk_threshold or sign(w13*vx1) < 0) then mu_sl*Fz13*
   cos(atan2(-v13y,(r*w13 - vx1))) else Fz13*((CCx*sx13*o13^2) + (
   mu_sl*cos(atan2(-v13y,(r*w13 - vx1)))*(1-3*o13^2+2*o13^3)));
sx13 = (r*w13 - vx1)/abs(r*w13) "Longitudinal slip at the third axle";

sk11 = sqrt((k*sx11)^2 + sy11^2);
sk12 = sqrt((k*sx12)^2 + sy12^2);
sk13 = sqrt((k*sx13)^2 + sy13^2);

s11 = sqrt(sx11^2 + sy11^2) "Combined slip at the first axle";
s12 = sqrt(sx12^2 + sy12^2) "Combined slip at the second axle";
s13 = sqrt(sx13^2 + sy13^2) "Combined slip at the third axle";

v1fxw = vx1*cos(steer) + v11y*sin(steer);
v1fyw = -vx1*sin(steer) + v11y*cos(steer);
v11y = vy1 + wz1*lf1;
v12y = vy1 - wz1*(lr1 - 0.685);
v13y = vy1 - wz1*(lr1 + 0.685);
v11cy = vy1 - wz1*(l1c-lf1);

Fy11 = if sk11 > sk_threshold then -1*mu_sl*Fz11*sin(atan2(-v1fyw,(r*
   w11 - v1fxw))) else -1*(Fz11*((CCy*sy11*o11^2) - sin(atan2(-v1fyw
   ,(r*w11 - v1fxw)))*(mu_sl*(1-3*o11^2+2*o11^3))));
Fy12 = if sk12 > sk_threshold then -1*mu_sl*Fz12*sin(atan2(-v12y,(r*
   w12 - vx1))) else -1*(Fz12*((CCy*sy12*o12^2) - sin(atan2(-v12y,(r*
   w12 - vx1)))*(mu_sl*(1-3*o12^2+2*o12^3))));
Fy13 = if sk13 > sk_threshold then -1*mu_sl*Fz13*sin(atan2(-v13y,(r*
   w13 - vx1))) else -1*(Fz13*((CCy*sy13*o13^2) - sin(atan2(-v13y,(r*
   w13 - vx1)))*(mu_sl*(1-3*o13^2+2*o13^3))));

der(x1) = vx1*cos(phi_1) - vy1*sin(phi_1) "x-coordinate of the tractor
   ";
der(y1) = vy1*cos(phi_1) + vx1*sin(phi_1) "y-coordinate of the tractor
   ";
der(phi_1) = wz1;

//------------------------ Equations of motion of Semi-Trailer 1
   --------------------------- //

m2*(der(vx2) - wz2*vy2) = (Fx21 + Fx22 + Fx23) + P2x + P3x - m2*g*sin(
   slope) "Longitudinal force equilibrium";
m2*(der(vy2) + wz2*vx2) = (Fy21 + Fy22 + Fy23) + P2y + P3y "Lateral
   force equilibrium";
i2*der(wz2) = -(dr21*Fy21 + dr22*Fy22 + dr23*Fy23) + P2y*lf2 - P3y*
   la22c "Yaw equilibrium";

ay2 = der(vy2) + wz2*vx2 "Lateral acceleration of the first semi-
   trailer";
R2 = if wz2 == 0 then 0 else abs(sqrt(vx2^2 + vy2^2))/wz2 "Radius of
   curvature"; //Valid for steady state cornering only

o21 = 1 - ((sk21*CCy)/(3*mu_st));
o22 = 1 - ((sk22*CCy)/(3*mu_st));
```

```
o23 = 1 - ((sk23*CCy)/(3*mu_st));

// Change the definition of lateral slips
   ..................................................
Fy21 = if (sk21 > sk_threshold or sign(w21*vx2) < 0) then -1*mu_sl*
   Fz21*sin(atan2(-v21y,(r*w21 - vx2))) else -1*(Fz21*((CCy*sy21*o21
   ^2) - sin(atan2(-v21y,(r*w21 - vx2)))*(mu_sl*(1-3*o21^2+2*o21^3)))
   );
Fy22 = if (sk22 > sk_threshold or sign(w22*vx2) < 0) then -1*mu_sl*
   Fz22*sin(atan2(-v22y,(r*w22 - vx2))) else -1*(Fz22*((CCy*sy22*o22
   ^2) - sin(atan2(-v22y,(r*w22 - vx2)))*(mu_sl*(1-3*o22^2+2*o22^3)))
   );
Fy23 = if (sk23 > sk_threshold or sign(w23*vx2) < 0) then -1*mu_sl*
   Fz23*sin(atan2(-v23y,(r*w23 - vx2))) else -1*(Fz23*((CCy*sy23*o23
   ^2) - sin(atan2(-v23y,(r*w23 - vx2)))*(mu_sl*(1-3*o23^2+2*o23^3)))
   );

sy21 = v21y/abs(r*w21) "Lateral slip at the first axle";
sy22 = v22y/abs(r*w22) "Lateral slip at the second axle";
sy23 = v23y/abs(r*w23) "Lateral slip at the third axle";

sk21 = sqrt((k*sx21)^2 + sy21^2);
sk22 = sqrt((k*sx22)^2 + sy22^2);
sk23 = sqrt((k*sx23)^2 + sy23^2);

s21 = sqrt((sx21)^2 + sy21^2) "Combined slip at the first axle";
s22 = sqrt((sx22)^2 + sy22^2) "Combined slip at the first axle";
s23 = sqrt((sx23)^2 + sy23^2) "Combined slip at the first axle";

Tap21 = Jwh*der(w21) + Fx21*r + rrc*Fz21*sign(vx2) "Wheel torque
   equilibrium for first axle";
Fx21 = if (sk21 > sk_threshold or sign(w21*vx2) < 0) then mu_sl*Fz21*
   cos(atan2(-v21y,(r*w21 - vx2))) else Fz21*((CCx*sx21*o21^2) + (
   mu_sl*cos(atan2(-v21y,(r*w21 - vx2)))*(1-3*o21^2+2*o21^3)));
sx21 = (r*w21 - vx2)/abs(r*w21) "Longitudinal slip at the first axle";

Tap22 = Jwh*der(w22) + Fx22*r + rrc*Fz22*sign(vx2) "Wheel torque
   equilibrium for second axle";
Fx22 = if (sk22 > sk_threshold or sign(w22*vx2) < 0) then mu_sl*Fz22*
   cos(atan2(-v22y,(r*w22 - vx2))) else Fz22*((CCx*sx22*o22^2) + (
   mu_sl*cos(atan2(-v22y,(r*w22 - vx2)))*(1-3*o22^2+2*o22^3)));
sx22 = (r*w22 - vx2)/abs(r*w22) "Longitudinal slip at the second axle
   ";

Tap23 = Jwh*der(w23) + Fx23*r + rrc*Fz23*sign(vx2) "Wheel torque
   equilibrium for third axle";
Fx23 = if (sk23 > sk_threshold or sign(w23*vx2) < 0) then mu_sl*Fz23*
   cos(atan2(-v23y,(r*w23 - vx2))) else Fz23*((CCx*sx23*o23^2) + (
   mu_sl*cos(atan2(-v23y,(r*w23 - vx2)))*(1-3*o23^2+2*o23^3)));
sx23 = (r*w23 - vx2)/abs(r*w23) "Longitudinal slip at the third axle";

v21y = vy2 - wz2*dr21;
v22y = vy2 - wz2*dr22;
v23y = vy2 - wz2*dr23;
```

```
v12cy = vy2 + wz2*lf2 "Lateral velocity of the first coupling point in
    terms of semi-trailer 1";
v22cy = vy2 - wz2*la22c "Lateral velocity of the second coupling point
    in terms of semi-trailer 1";

P1x + P2x*cos(theta_1) + P2y*sin(theta_1) = 0;
P1y - P2x*sin(theta_1) + P2y*cos(theta_1) = 0;

vx1 = vx2*cos(theta_1) + v12cy*sin(theta_1);
v11cy = -vx2*sin(theta_1) + v12cy*cos(theta_1);
der(theta_1) = wz1-wz2;

der(x2) = vx2*cos(phi_2) - vy2*sin(phi_2);
der(y2) = vy2*cos(phi_2) + vx2*sin(phi_2);
der(phi_2) = wz2;

//// --------------- Equations of motion of dolly
   ------------------////
m3*(der(vx3) - wz3*vy3) = (Fx31 + Fx32) + P4x + P5x - m3*g*sin(slope)
   "Longitudinal force equilibrium";
m3*(der(vy3) + wz3*vx3) = (Fy31 + Fy32) + P4y + P5y "Lateral force
   equilibrium";
i3*der(wz3) = (dr31*Fy31 - dr32*Fy32) + P4y*lac32 - P5y*lac34 "Yaw
   equilibrium";

ay3 = der(vy3) + wz3*vx3 "Lateral acceleration of the e-dolly";
R3 = if wz3 == 0 then 0 else abs(sqrt(vx3^2 + vy3^2))/wz3 "Radius of
   curvature"; //Valid for steady state cornering only;

o31 = 1 - ((sk31*CCy)/(3*mu_st));
o32 = 1 - ((sk32*CCy)/(3*mu_st));

Jwh*der(w31) = Tap31 - Fx31*r - rrc*Fz31*sign(vx3) "Wheel torque
   equilibrium for the first axle of e-dolly";
Fx31 = if (sk31 > sk_threshold or sign(w31*vx3) < 0) then mu_sl*Fz31*
   cos(atan2(-v31y,(r*w31 - vx3))) else Fz31*((CCx*sx31*o31^2) + (
   mu_sl*cos(atan2(-v31y,(r*w31 - vx3)))*(1-3*o31^2+2*o31^3)));
sx31 = (r*w31 - vx3)/abs(r*w31);

Jwh*der(w32) = Tap32 - Fx32*r - rrc*Fz32*sign(vx3) "Wheel torque
   equilibrium for the second axle of e-dolly";
Fx32 = if (sk32 > sk_threshold or sign(w32*vx3) < 0) then mu_sl*Fz32*
   cos(atan2(-v32y,(r*w32 - vx3))) else Fz32*((CCx*sx32*o32^2) + (
   mu_sl*cos(atan2(-v32y,(r*w32 - vx3)))*(1-3*o32^2+2*o32^3)));
sx32 = (r*w32 - vx3)/abs(r*w32);

fu32 = sqrt((Fx32)^2 + (Fy32)^2)/max_f32 "Coefficient of friction
   usage at the second (driven) axle of e-dolly";
max_f32 = Fz32*mu_peak "Max force available at the second axle";

fu31 = sqrt((Fx31)^2 + (Fy31)^2)/max_f31 "Coefficient of friction
   usage at the first axle of e-dolly";
max_f31 = Fz31*mu_peak "Max force available at the first axle";

Fy31 = if (sk31 > sk_threshold or sign(w31*vx3) < 0) then -1*mu_sl*
   Fz31*sin(atan2(-v31y,(r*w31 - vx3))) else -1*(Fz31*((CCy*sy31*o11
```

```
    ^2) - sin(atan2(-v31y,(r*w31 - vx3)))*(mu_sl*(1-3*o31^2+2*o31^3)))
    );
Fy32 = if (sk32 > sk_threshold or sign(w32*vx3) < 0) then -1*mu_sl*
    Fz32*sin(atan2(-v32y,(r*w32 - vx3))) else -1*(Fz32*((CCy*sy32*o12
    ^2) - sin(atan2(-v32y,(r*w32 - vx3)))*(mu_sl*(1-3*o32^2+2*o32^3)))
    );

sy31 = v31y/abs(r*w31) "Lateral slip at the first axle";
sy32 = v32y/abs(r*w32) "Lateral slip at the second axle";

sk31 = sqrt((k*sx31)^2 + sy31^2);
sk32 = sqrt((k*sx32)^2 + sy32^2);

s31 = sqrt((sx31)^2 + sy31^2) "Combined slip at the first axle";
s32 = sqrt((sx32)^2 + sy32^2) "Combined slip at the second axle";

v31y = vy3 + wz3*dr31;
v32y = vy3 - wz3*dr32;

v23cy = vy3 + wz3*lac32 "Lateral velocity of the second coupling point
     in terms of e-dolly";
v33cy = vy3 - wz3*lac34 "Lateral velocity of the third coupling point
    in terms of e-dolly";

P3x + P4x*cos(theta_2) + P4y*sin(theta_2) = 0;
P3y - P4x*sin(theta_2) + P4y*cos(theta_2) = 0;

vx2 = vx3*cos(theta_2) + v23cy*sin(theta_2);
v22cy = -vx3*sin(theta_2) + v23cy*cos(theta_2);
der(theta_2) = wz2-wz3;

der(x3) = vx3*cos(phi_3) - vy3*sin(phi_3);
der(y3) = vy3*cos(phi_3) + vx3*sin(phi_3);
der(phi_3) = wz3;


// -------------TRAILER 2--------------- //
m4*(der(vx4) - wz4*vy4) = (Fx41 + Fx42 + Fx43) + P6x - m4*g*sin(slope)
     "Longitudinal force equilibrium";
m4*(der(vy4) + wz4*vx4) = (Fy41 + Fy42 + Fy43) + P6y "Lateral force
    equilibrium";
i4*der(wz4) = -(dr41*Fy41 + dr42*Fy42 + dr43*Fy43) + P6y*lf4 "Yaw
    equilibrium";

ay4 = der(vy4) + wz4*vx4 "Lateral acceleration of the second semi-
    trailer";
R4 = if wz4 == 0 then 0 else abs(sqrt(vx4^2 + vy4^2))/wz4 "Radius of
    curvature"; //Valid for steady state cornering only;

o41 = 1 - ((sk41*CCy)/(3*mu_st));
o42 = 1 - ((sk42*CCy)/(3*mu_st));
o43 = 1 - ((sk43*CCy)/(3*mu_st));

Fy41 = if (sk41 > sk_threshold or sign(w41*vx4) < 0) then -1*mu_sl*
    Fz41*sin(atan2(-v41y,(r*w41 - vx4))) else -1*(Fz41*((CCy*sy41*o41
    ^2) - sin(atan2(-v41y,(r*w41 - vx4)))*(mu_sl*(1-3*o41^2+2*o41^3)))
```

```
    );
Fy42 = if (sk42 > sk_threshold or sign(w42*vx4) < 0) then -1*mu_sl*
    Fz42*sin(atan2(-v42y,(r*w42 - vx4))) else -1*(Fz42*((CCy*sy42*o42
    ^2) - sin(atan2(-v42y,(r*w42 - vx4)))*(mu_sl*(1-3*o42^2+2*o42^3)))
    );
Fy43 = if (sk43 > sk_threshold or sign(w43*vx4) < 0) then -1*mu_sl*
    Fz43*sin(atan2(-v43y,(r*w43 - vx4))) else -1*(Fz43*((CCy*sy43*o43
    ^2) - sin(atan2(-v43y,(r*w43 - vx4)))*(mu_sl*(1-3*o43^2+2*o43^3)))
    );

Jwh*der(w41) = Tap41 - Fx41*r - rrc*Fz41*sign(vx4) "Wheel torque
    equilibrium for the first axle of Semi-trailer 2";
Fx41 = if (sk41 > sk_threshold or sign(w41*vx4) < 0) then mu_sl*Fz41*
    cos(atan2(-v41y,(r*w41 - vx4))) else Fz41*((CCx*sx41*o41^2) + (
    mu_sl*cos(atan2(-v41y,(r*w41 - vx4)))*(1-3*o41^2+2*o41^3)));
sx41 = (r*w41 - vx4)/abs(r*w41);

Jwh*der(w42) = Tap42 - Fx42*r - rrc*Fz42*sign(vx4) "Wheel torque
    equilibrium for the second axle of Semi-trailer 2";
Fx42 = if (sk42 > sk_threshold or sign(w42*vx4) < 0) then mu_sl*Fz42*
    cos(atan2(-v42y,(r*w42 - vx4))) else Fz42*((CCx*sx42*o42^2) + (
    mu_sl*cos(atan2(-v42y,(r*w42 - vx4)))*(1-3*o42^2+2*o42^3)));
sx42 = (r*w42 - vx4)/abs(r*w42);

Jwh*der(w43) = Tap43 - Fx43*r - rrc*Fz43*sign(vx4) "Wheel torque
    equilibrium for the third axle of Semi-trailer 2";
Fx43 = if (sk43 > sk_threshold or sign(w43*vx4) < 0) then mu_sl*Fz43*
    cos(atan2(-v43y,(r*w43 - vx4))) else Fz43*((CCx*sx43*o43^2) + (
    mu_sl*cos(atan2(-v43y,(r*w43 - vx4)))*(1-3*o43^2+2*o43^3)));
sx43 = (r*w43 - vx4)/abs(r*w43);

sy41 = v41y/abs(r*w41) "Lateral slip at the first axle";
sy42 = v42y/abs(r*w42) "Lateral slip at the second axle";
sy43 = v43y/abs(r*w43) "Lateral slip at the third axle";

fu43 = sqrt((Fx43)^2 + (Fy43)^2)/max_f43;
max_f43 = Fz43*mu_peak;

sk41 = sqrt((k*sx41)^2 + sy41^2);
sk42 = sqrt((k*sx42)^2 + sy42^2);
sk43 = sqrt((k*sx43)^2 + sy43^2);

s41 = sqrt((sx41)^2 + sy41^2) "Combined slip at the first axle";
s42 = sqrt((sx42)^2 + sy42^2) "Combined slip at the second axle";
s43 = sqrt((sx43)^2 + sy43^2) "Combined slip at the third axle";

v41y = vy4 - wz4*dr41;
v42y = vy4 - wz4*dr42;
v43y = vy4 - wz4*dr43;

v34cy = vy4 + wz4*lf4 "Lateral velocity of the third coupling point in
    terms of Semi-trailer 2";

P5x + P6x*cos(theta_3) + P6y*sin(theta_3) = 0;
P5y - P6x*sin(theta_3) + P6y*cos(theta_3) = 0;
```

```
 vx3 = vx4*cos(theta_3) + v34cy*sin(theta_3);
 v33cy = -vx4*sin(theta_3) + v34cy*cos(theta_3);
 der(theta_3) = wz3-wz4;

 der(x4) = vx4*cos(phi_4) - vy4*sin(phi_4);
 der(y4) = vy4*cos(phi_4) + vx4*sin(phi_4);
 der(phi_4) = wz4;
  annotation (experiment(StopTime=40, __Dymola_Algorithm="Dassl"));
end Deceleration_in_a_curve;
```

DEPARTMENT OF MECHANICS AND MARITIME SCIENCES
CHALMERS UNIVERSITY OF TECHNOLOGY
Gothenburg, Sweden
www.chalmers.se

CHALMERS
UNIVERSITY OF TECHNOLOGY